Copy No. _____

Defence Research and Development Canada
Recherche et développement pour la défense Canada

DEFENCE R&D DÉFENSE

A Novel Detector of Broadband Transient Signals

Jüri Sildam

Defence R&D Canada – Atlantic

Technical Memorandum
DRDC Atlantic TM 2006-258
November 2006

Canada

This page intentionally left blank.

A Novel Detector of Broadband Transient Signals

Jüri Sildam

Defence R&D Canada – Atlantic
Technical Memorandum
DRDC Atlantic TM 2006-258
November 2006

Principal Author

Jüri Sildam

Approved by

David Hazen
Head/Technology Demonstration

Approved for release by

Kirk Foster
Chair/Document Review Panel

Abstract

A novel approach for detection of broad-band (BB) transients (DBBT) is proposed. DBBT is based on an analysis of the spectrograms, calculated from time series of one or more hydrophones. A spectrogram is divided into locally normalized time-frequency cells (TFC). Two TFCs, which are measured at the same time but at different neighboring frequencies, are said to include a signature of a broad-band transient signal if their empirical centres of masses estimated in a higher-dimensional feature space using a Gaussian kernel exhibit correlation higher than a predefined threshold. A spread coefficient p of a Gaussian kernel is chosen so that the correlation between the pairs of centres of masses of TFCs that do not include transient signatures appear to be uncorrelated. Tests of BB transient detection, carried out using a number of real-world data sets, demonstrate robustness of the proposed method. In particular, DBBT was able to detect the launch and explosion of a torpedo, the start and stop of small boat engine, and other events. Reusable values of size of TF cells, a p value, and correlation threshold were used. The same settings were also successfully used with two sets of torpedo and ship measurements artificially combined at different bearings within a framework of simulated beam-forming. The results were found to be relatively insensitive to the array shape and target bearing errors. A few tests that were carried out on artificially generated narrowband signals using modified DBBT were found to be too limited and therefore inconclusive.

Résumé

On propose une nouvelle méthode de détection de transitoires à large bande (DBBT). La méthode DBBT est basée sur une analyse des spectrogrammes, obtenus à partir de séries chronologiques d'un ou de plusieurs hydrophones. Un spectrogramme est divisé en cellules temps-fréquence (TFC) normalisées localement. On dit de deux TFC mesurées à la même heure mais à des fréquences voisines différentes qu'elles contiennent une signature de signal transitoire à large bande si leurs centres de masse empiriques estimés dans un espace de caractéristiques à plus grand nombre de dimensions à l'aide d'un noyau gaussien présentent une corrélation supérieure à un seuil prédéfini. Un coefficient d'étalement p d'un noyau gaussien est choisi de façon que les paires de centres de masse des TFC qui ne contiennent pas de signatures transitoires semblent non corrélées. Des essais de détection de transitoires à large bande, effectués avec un certain nombre d'ensembles de données réels, montrent la robustesse de la méthode proposée. En particulier, la méthode DBBT a permis de détecter le lancement et l'explosion d'une torpille, le démarrage et l'arrêt d'un moteur de petite embarcation, de même que d'autres événements. Des valeurs réutilisables de la taille de cellules temps-fréquence, une valeur de p et un seuil de corrélation ont été utilisés. Les mêmes réglages ont aussi été utilisés avec succés avec deux ensembles de mesures relatives à des torpilles et des navires combinées artificiellement à différents relévements dans un cadre de mise en forme de faisceau simulée. On a constaté

que les résultats étaient relativement indépendants de la forme du réseau et des erreurs de relévement des cibles. On a constaté que quelques essais effectués sur des signaux à bande étroite générés artificiellement, à l'aide d'une version modifiée de la méthode DBBT, étaient trop limités et par conséquent non concluants.

Executive summary

A Novel Detector of Broadband Transient Signals

Jüri Sildam; DRDC Atlantic TM 2006-258; Defence R&D Canada – Atlantic; November 2006.

Introduction: Detection of transients (e.g. a torpedo entering the water), can be seen as a first step in target detection, localization, and classification problem. The non-stationarity of acoustical signal measured during a transient event makes detection of the transient a challenging task. For example, one may need to detect a transient against the background of relatively loud non-stationary and non-Gaussian noise created by one or more moving ships. The present work proposes a novel approach to the problem of detection of broadband transients.

Results: The proposed of detection of broad-band transients (DBBT) is based on analysis of the spectrograms, calculated from time-series of one or more hydrophones. DBBT is able to detect the transients that manifest themselves as a sudden increase in spectral energy observed in a short time over a broad band of frequencies. In contrast to the approaches of transient detection, which $directly$ test the signal changes in time, DBBT tests for similarity of time-frequency cells along a frequency axis to decide whether there were any significant changes in time. Tests of BB transient detection, carried out using a number of real-world data sets, demonstrate robustness of the proposed method.

Significance of results: The proposed approach can be used for detection of BB transients in a number of different applications where transients manifest themselves as a sudden increase in spectral energy observed over a short time in a broad band of frequencies. This algorithm is potentially useful for torpedo detection under the Multi-Sensor Torpedo DCL TDP as well as in Marine Mammal detection and general transient-based submarine detection.

Future work:

1. The approach will be tested against recorded data collected as part of the MSTDCL TDP
2. If the approach shows promise, the approach will be coded into a Transient Detection module for the System Test Bed (STB)

Sommaire

A Novel Detector of Broadband Transient Signals

Jüri Sildam; DRDC Atlantic TM 2006-258; Defence R&D Canada – Atlantic; novembre 2006.

Introduction: : La détection de transitoires (p. ex. lorsqu'une torpille entre dans l'eau) peut être considérée comme une première étape de la résolution du problme de détection, localisation et classification des cibles. La non-stationnarité du signal acoustique mesuré durant un événement transitoire complique la détection du transitoire. Par exemple, il peut être nécessaire de détecter un transitoire en présence d'un bruit de fond non stationnaire et non gaussien relativement élevé créé par un ou plusieurs navires en déplacement. Le présent document propose une nouvelle méthode de résolution du problme de détection de transitoires à large bande.

Résultats: : La méthode proposée de détection des transitoires à large bande (DBBT) est basée sur l'analyse de spectrogrammes, obtenus à partir de séries chronologiques d'un ou de plusieurs hydrophones. La méthode DBBT permet de détecter les transitoires qui se manifestent sous forme d'un accroissement soudain de l'énergie spectrale observé pendant une courte période sur une vaste gamme de fréquences. Contrairement aux autres méthodes de détection des transitoires, qui cherchent à déterminer directement les variations du signal dans le temps, la méthode DBBT cherche à déterminer la similarité des cellules temps fréquence suivant un axe de fréquences pour déterminer s'il s'est produit des variations appréciables dans le temps. Des essais de détection de transitoires à large bande, effectués avec un certain nombre d'ensembles de données réels, montrent la robustesse de la méthode proposée.

Portée: : La méthode proposée peut être utilisée pour la détection de transitoires à large bande dans un certain nombre d'applications différentes dans lesquelles les transitoires se manifestent sous forme d'un accroissement soudain de l'énergie spectrale observé pendant une courte période sur une vaste gamme de fréquences. L'algorithme de cette méthode pourrait être utile pour la détection de torpilles dans le cadre du projet de démonstration de technologie de détection, de classification et de localisation de torpilles à partir de capteurs multiples (PDT MSTDCL), de même que pour la détection de mammifères marins et la détection générale de sous-marins basée sur les transitoires.

Recherches futures: :

1. La méthode sera testée avec des données enregistrées recueillies dans le cadre du PDT MSTDCL.

2. Si elle se révle prometteuse, la méthode sera codée sous forme d'un module de détection de transitoires pour le banc d'essai de système (STB).

This page intentionally left blank.

Table of contents

List of figures

Acknowledgements

The author would like thank Dr. Mark Trevorrow for a number of useful suggestions, and Mr. Howie Nippard for pointing out a website where the recordings of acoustical signatures are made available to the general public.

1 Introduction

A transient is an acoustic event of short duration that causes significant changes in an acoustic environment. From a point of view of a target detection, classification, and localization (DCL), transient detection can be seen as a first step in target DCL (e.g. a torpedo entering the water). Non-stationarity of acoustical signal measured in background prior, during-, and after of a transient event, makes detection of the transient a challenging task. For example, one may need to detect a transient at the background of relatively loud non-stationary and non-Gaussian noise caused by one or more moving ships. For known signal and noise distributions, a transient detection becomes a classical test for detection of statistical change such as Generalized Likelihood Ratio (GLR) test or Page's CUSUM test ([1, 2]). Time-frequency representations are often used for analysis of non-stationary signals. In particular, spectrograms can be segmented using local statistical properties of time-frequency cells (TFCs) [3, 4]. When the underlying distributions are unknown or when an accurate signal model is unavailable, model-free approaches should be considered [5]. The present work follows the latter path. It can be used in an automation of BB transient detection, which is one of the goals of Multi-sensor Torpedo Detection, Classification, and Localization TDP, carried out by DRDC-Atlantic.

A brief description of the problem, its formulation, and a proposed solution for detection of broadband (BB) transients is presented in the next section (more details on model-free novelty detection in the context of present work can be found in the companion report [6]). The proposed technique is applied then to a number of real-world acoustic data-sets available at WWW sites [7] and [8]. For sake of completeness, two real-world examples (torpedo launch, run, and target hit, and noise of a ship) are taken, and artificially mixed as they would have been observed by an array of hydrophones freely towed behind a vessel. Robustness of the proposed approach is tested by introduction of errors in array shape and in target bearing estimation. Finally, a discussion of results and summary of conclusions is provided.

2 Detection of Broad-Band Transient Signals

2.1 Framework of Non-parametric Detection of Transients

Transient detection is based on estimation of some dissimilarity measure D between two successive data sets $\mathbf{y_i}$ and $\mathbf{y_{i+1}}$. The respective sets can be obtained by arranging time-series of a measured parameter y_t or descriptors x_t estimated from the time-series y_t (in what follows the upper bold, lower bold, and lower letters will stand for a vector, a matrix, and a scalar respectively). Under a zero hypothesis (H_0), two successive sets $\mathbf{y_i}$ and $\mathbf{y_{i+1}}$ are said to be similar if a chosen dissimilarity measure does not exceed a preset threshold η. In an opposite case (here in a case of transient), a hypothesis H_1 is said to be true:

$$\begin{cases} H_0 : D(\mathbf{y_i}, \mathbf{y_{i+1}}) \leq \eta, \\ H_1 : D(\mathbf{y_i}, \mathbf{y_{i+1}}) > \eta \end{cases} \tag{1}$$

For a purpose of the following analysis, we arrange the sets of original time-series $\mathbf{y_i} = [y_{t_0}, ..., y_{t_N}]^T$ (here T means transpose) into matrices $\mathbf{Y} = [\mathbf{y_i}, ..., \mathbf{y_N}]$. The last equality can be written equivalently in a full matrix form:

$$\mathbf{Y} = \begin{bmatrix} y_{1,1} & y_{1,2} & \cdots & y_{1,L} \\ y_{2,1} & y_{2,2} & \cdots & y_{2,L} \\ \vdots & \vdots & & \vdots \\ y_{N,1} & y_{N,2} & \cdots & y_{N,L} \end{bmatrix} \tag{2}$$

By applying a column-wise magnitude-square FFT to equation (2) one obtains the matrix representation of a spectrogram:

$$\mathbf{X} = \begin{bmatrix} x_{1,1} & x_{1,2} & \cdots & x_{1,L} \\ x_{2,1} & x_{2,2} & \cdots & x_{2,L} \\ \vdots & \vdots & & \vdots \\ x_{N,1} & x_{N,2} & \cdots & x_{N,L} \end{bmatrix} \tag{3}$$

Similarly to the dissimilarity tests carried out in time domain (equation 1), dissimilarity analysis can be carried out in time-frequency domain. In this case, two spectra estimated at two consecutive mean time values can also be compared in terms of their similarity. It is straightforward to extend the respective analysis so that the tests will be carried out on two successive sets of spectra instead of a pair of spectra. For example, $\mathbf{X}$ in equation (3) can be divided into two parts, the first consisting of $1, ..., L/2$, and the second consisting of $L/2+1, ..., L$ spectra i.e. $\mathbf{X_1} = [\mathbf{x_1}, \mathbf{x_2}, ..., \mathbf{x_{L/2}}]$ and $\mathbf{X_2} = [\mathbf{x_{L/2+1}}, \mathbf{x_{L/2+2}}, ..., \mathbf{x_L}]$, where $\mathbf{x_j} = [x_{1,j}, ..., x_{N,j}]^T, j = 1, ..., L$. Now, the dissimilarity test can be written as:

$$\begin{cases} H_0 : D(\mathbf{X_1}, \mathbf{X_2}) \leq \eta, \\ H_1 : D(\mathbf{X_1}, \mathbf{X_2}) > \eta \end{cases} \tag{4}$$

2.2 Kernel Based Similarity Measure in the Context of Support Vector Machines

In recent decade, the machine learning approaches based on kernel methods for pattern analysis have been widely used (see e.g. [9]). In this framework the problem of transient detection based on a limited amount of data can be addressed via a single class classification problem. In the context of our spectral data, the underlying idea in its simplest form is to map input spectral data $\phi(\mathbf{x})$ into some higher dimensional feature space $\mathcal{F}$ where it can be enclosed into a hyper-sphere. The volume of this hyper-sphere can be minimized so that it would include most of the data points of a single class defined by a set of measured spectra. In $\mathcal{F}$ the distance from the hyper-sphere can be then estimated for any newly measured data $\phi(\mathbf{z})$ in terms of its novelty (novel data would lie outside the hyper-sphere). A so called kernel trick is introduced to avoid computationally expensive explicit data mapping. A kernel matrix $\mathbf{K}(\mathbf{j},\mathbf{i})$ provides inner product information evaluated between all pairs of elements of $\mathbf{X}$:.

$$k(\mathbf{x_j},\mathbf{x_i}) =< \phi(\mathbf{x_j}),\phi(\mathbf{x_i}) > \tag{5}$$

As a result of use of a Gaussian kernel,

$$k(\mathbf{x_j},\mathbf{x_i}) = e^{(-\frac{||x_i - x_j||^2}{p})} \tag{6}$$

spectral data is mapped on to a hyper-sphere and $k(\mathbf{x_i},\mathbf{x_i}) = 1$. Therefore, use of a Gaussian kernel changes geometrical interpretation of novelty detection, which can be shown using the following example. Figure 1 shows an example of two data sets of points (black dots) located on the surface of three-dimensional sphere. The two sets can be distinguished by two green thick circles surrounding the respective sets. For clarity the smaller data set can be dismissed for now. Color of the sphere surface corresponds to the relative distance values from the green circle of the bigger data set on the right side of the Figure. The regions inside and outside of the bigger circle correspond to positive and negative distances respectively. One can see that the absolute value of negative distance increases as one moves away from the bigger circle. These distances as well as the green circle around the bigger data set were obtained as result of a solution of one-class problem based on support vector machines (SVM). Although SVM was not used in the present work, to put the approach used in this work into a proper context, a short description of the SVM approach for one class problem is given below.

One could think of the example shown in Figure 1 as a N dimensional hyper-sphere, with the data points that lie on its surface as the spectra that had been mapped into $\mathcal{F}$. According to the SVM approach ([9, 5]), the problem of novelty detection based on a Gaussian kernel (recall that in this case $k(\mathbf{x_i},\mathbf{x_i}) = 1$) is to find a hyper-plane, which divides the origin of the hyper-sphere and most of the data in $\mathcal{F}$ so that the distance between the hyper-plane and the origin would be maximized (for more details see [6]). In the present example, the thick green line would correspond then to the region of intersection

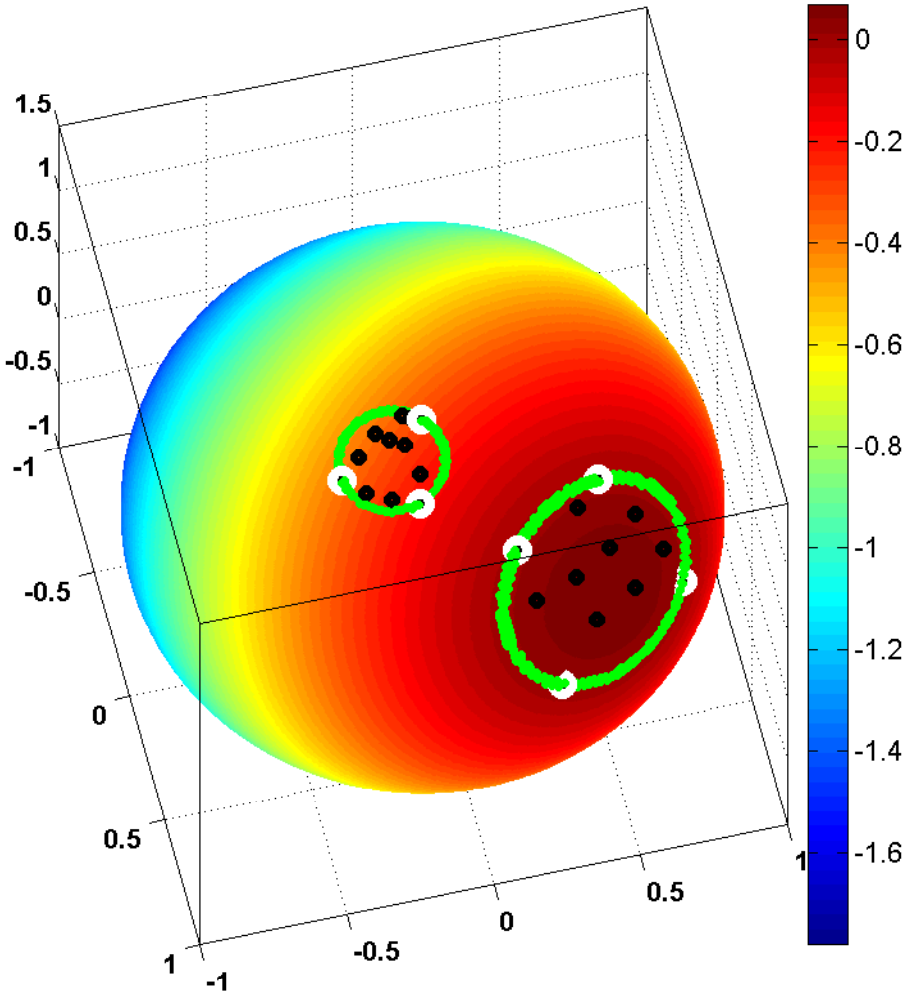

Figure 1: *An illustration of the two cases of novelty detection using the kernel based approaches. In the first case, the data set shown by the small black circles in the right of side of the sphere corresponds to one class. Color of the sphere corresponds to the distance from the decision boundary obtained from a solution one class SVM (green line). Any measurement that lies outside or inside this decision boundary would be called a novel or belonging to this class respectively. In the first case the smaller data set seen in the left side was not used to obtain the decision boundary seen in the right. In the second case, another decision boundary was obtained from a solution one class SVM (green circle in the left) independently of the data seen in the right side. In the second case, a novelty index can be obtained as an arc distance between the two centres of masses of the two data sets without using SVM. The white small circles on the top of the decision boundaries of both data-sets represent support vectors and are shown only for illustration purposes. They were obtained by solving a linear SVM problem for each of the data-sets.*

of the hyper-plane (which is not shown) with the hyper-sphere. Depending whether all data points have to lie within the given circle or some outliers are allowed to lie outside of the green circle, SVMs and other kernel based approaches are divided into hard- and soft margin classifiers respectively. For the purpose of the present example it is sufficient to consider only the hard-margin classifiers. The white small circles that lie right on the green line correspond to the data points that define the intersection of the hyper-plane with the hyper-sphere. The respective data vectors are called support vectors. In the context of spectra based on acoustical measurements, the set of data points shown in Figure 1 could correspond to the spectra estimated at the time interval $t + \delta t$. The support vectors would correspond then to the spectra that define the decision boundary (given by green line) around the given set (according to Vapnik, instead of trying to address a difficult problem of estimation of probability distribution function (PDF), one may address an easier problem of estimating the support of underlying PDF). Now, any new measured spectrum could be estimated in terms of its novelty (i.e. in terms of the distance from the decision boundary of the larger data set). Another way for novelty detection would be to collect a new set of measured spectra and to compare it with the set collected previously. Such a situation is depicted in Figure 1. In [5] a dissimilarity measure D between a pair of data sets was obtained by solving a one class classification problem separately for both data sets, followed by estimation of a ratio of an arc distance between the empirical centres of masses of the two data-sets and a sum of arc distances between the respective centres of masses and their support vectors. For purpose of the present problem formulation, however, a simpler and importantly computationally faster approach is used. Namely, instead of estimating support of an underlying pdf, in $\mathcal{F}$ only an arc distance between the empirical centres of the respective masses of the data sets $\mathbf{X_i}$ and $\mathbf{X_{i+1}}$ is used. It may seem to be a significant disadvantage not to consider a spread of data in $\mathcal{F}$. However, as it will be seen below, by limiting our solution only to a certain type transients, we obtain a sort of filtered approach that would effectively suppress other types of events, making the similarity measure less noisy, and making it easier to come up with a required threshold. So when a norm of a Gaussian kernel $||\mathbf{x_i} - \mathbf{x_j}|| \gg p$ then $K(\mathbf{x_i}, \mathbf{x_j}) \to 0$, and in an opposite case if $||\mathbf{x_i} - \mathbf{x_j}|| \ll p$ then $K(\mathbf{x_i}, \mathbf{x_j}) \to 1$. The correlation of the two centres of masses in a higher dimensional feature space equals to:

$$r = \frac{\sum_{i,j} K(x_i, z_j)}{\sqrt{\sum_{i,j} K(x_i, x_j)} \sqrt{\sum_{i,j} K(z_i, z_j)}} \tag{7}$$

Note that in a context of this work $\mathbf{x_i}$ and $\mathbf{z_i}$ stay for the spectra of the first and second data sets respectively (or vice versa). Note also that equation 7 corresponds to the ν-SVM one-class decision function built on the Parzen window estimate [5]. Thus, for a purpose of the present work $D = 1 - r$. The next section will give an another example, which will be followed then by the formulation of the test of transient detection using r.

2.3 Example 1. Problem Formulation

In equation 6 it is possible to choose so small spread factor p such that even when two datasets are obtained from an independent identical distribution (I.I.D.) (e.g. from a normal distribution with equal mean, and variance values), r is close to 0. In an event when variance significantly increases and becomes comparable to p, the estimate of r will tend to be close to 1. Thus by using a Gaussian kernel with a fixed spread factor p, one can detect the onset or end of the processes, which variances are comparable or higher than p. By itself such a result is not very interesting since it requires $a\ priori$ knowledge of variance values of underlying processes. However, one can make a problem solution invariant to data absolute energy levels by normalizing data sets by norms of the respective data-sets:

$$\hat{\mathbf{X}}_{\mathbf{k,l}} = \frac{\mathbf{X_{k,l}}}{\sqrt{\sum_{\mathbf{i,j}} \mathbf{X^2_{i,j}}}} \tag{8}$$

To show another useful aspect of this normalization, let us inspect an example shown in Figure 2. In this example, we generated non-stationary datasets using:

$$\mathbf{X_i} = \begin{bmatrix} g^2_{1,1} & \cdots & g^2_{1,L} \\ \vdots & & \vdots \\ g^2_{N,1} & \cdots & g^2_{N,L} \end{bmatrix} + s_i,\ \text{i=0,...,J-1} \tag{9}$$

$$\mathbf{X_i} = [\mathbf{X_1 X_2}],\ \text{i=J} \tag{10}$$

$$\text{where } \mathbf{X_1} = s_i + \begin{bmatrix} g^2_{1,1} & \cdots & g^2_{1,L/2} \\ \vdots & & \vdots \\ g^2_{N,1} & \cdots & g^2_{N,L/2} \end{bmatrix} \mathbf{X_2} = \begin{bmatrix} g^2_{1,L/2+1} & \cdots & g^2_{1,L} \\ \vdots & & \vdots \\ g^2_{N,L/2+1} & \cdots & g^2_{N,L} \end{bmatrix} 2s_i + s_i^2$$

$$\mathbf{X_i} = 2s_i \begin{bmatrix} g^2_{1,1} & \cdots & g^2_{1,L} \\ \vdots & & \vdots \\ g^2_{N,1} & \cdots & g^2_{N,L} \end{bmatrix} + s_i^2, \text{i=J+1,...,K} \tag{11}$$

where

$$s_i = s_1 + \frac{i(s_K - s_i)}{K-1}, i = 0, ..., K-2 \tag{12}$$

and $g_{i,j}$ is a random number drawn from the normal distribution with mean equal to 0 and standard deviation equal to 1. The constants used in equations [9], [10], [11], and [12] were set as follows: $s_1 = 1$, $s_K = 20$, $N = 200$ (dimension of a data vector), $K = 60$, $J = 15$, and $L = 70$. Index i can be interpreted here as an index of the average time when a dataset X_i was measured. Due to monotonically increasing s_i (and hence changing statistical moments

of $\mathbf{X_i}$), equations [9], [10], [11] represent non-stationary data-sets. In the present artificial simulation we have created the data sets under two statistical regimes at $t_{i<J}$ and at $t_{i>J}$ respectively, and one data set at $i = J$, capturing the end of the first and the start of the second regime. In order to detect the event at $t_i = J$, we ran the equations [9], [10], [11] twice with the only difference between $\mathbf{X_{i,1}}$ and $\mathbf{X_{i,2}}$ being the values of random numbers $g(l,k)$ drawn from the same normal distribution with mean 0, and variance 1. The distribution of standard deviation and mean of the data set pairs (black and red markers and lines) as a function s_i is shown in the panels B and C of Figure 2. Since the data set pairs were generated using I.I.D., the respective first and second moments, as expected, practically coincided,increasing as a function of s_i. A local peak at $s_i^2 = 36$ corresponds to the occurrence of a transient at $i = J$. Distribution of mean and standard deviation of normalized (using equation 8) data is shown in the panels D and E respectively. Note the significant changes of the respective mean and σ values at $i = J$. The angle between the two centres of masses is minimal (correlation is maximal) at $i = J$. Also the spread factor p multiplied by variance of normalized TFC exhibits a local peak at $s_i^2 = 36$ (Figure 3). The distribution of the first two components and histograms of all components of normalized data is shown in Figure 4. Inspecting this Figure one can see that the main difference between the histogram at $s_i^2 = 36$ and the rest of histograms is related to a number of peaks in the respective distributions. Whereas at $s_i^2 = 36$ two peaks can be observed, the rest of histograms show a single maximum. The top panel in the third column from the left shows similar information. One can see that both data sets are similarly distributed (red and black markers are almost on top of each other) with the two centres almost coinciding. Occurrence of the transient described by equation 10 can be now understood in a context of a relative change of spectral energy in time captured by both data sets $\mathbf{X_1}$ and $\mathbf{X_2}$. The transient manifests itself as an abrupt change in statistical properties of spectra observed from times $t_{j=1,\ldots,N/2}$ to times $t_{j=N/2+1,\ldots,N}$. In the case of a transient event, captured by both data-sets, the empirical centers of masses of the two data-sets in a feature space are highly correlated, and vice versa. Now, under the hypothesis H_0, a transient is not observed by any of the data sets $\mathbf{X_i}$, $\mathbf{X_{i+1}}$ if $r \leq r_\eta$. In the opposite case when a correlation between the respective pair of centres of masses in a feature space exceeds r_η, a transient is observed in both data sets. Thus the transient detection test can be written as:

$$\begin{cases} H_0 : \mathbf{X_1}, \mathbf{X_2} \text{ if } r(\mathbf{X_1}, \mathbf{X_2}) \leq r_\eta \\ H_1 : \mathbf{X_1}, \mathbf{X_2} \text{ if } r(\mathbf{X_1}, \mathbf{X_2}) > r_\eta \end{cases} \tag{13}$$

At first sight, it may seem that the dissimilarity test given by equation 4 contradicts to the respective test given by equation 13. However, it must be noted that in the former case a transient is captured by a significant change from one set to another whereas in the latter case a transient is captured by both data sets if they are similar to each other.

2.4 Example 2

In this section a recording of a ship-engine, which lasted about 10 seconds is used as somewhat artificial but a clear example. The length of this recording was artificially increased by using it repeatedly three times. Finally, to match the length of the torpedo recording (which will be used in the next section), Gaussian noise was appended to this modified ship-engine record. In this as well as in the all following examples the time series were divided into segments, each 1024 points long. The FFT was applied at each time segment without overlapping. The results were squared and divided into TFCs. Spectral data of each TFC was normalized using a local norm estimated separately for each TFC, which for the present examples consisted of 4 spectra each estimated at 6 frequencies. The width in time and in frequency of a TF cell was equal to 0.46 s and 75.4 Hz respectively. At each time instant in the spectrogram, equation 7 was applied pair-wise on all TF cells along a frequency axis. As the result, a distribution of r^2 was obtained as a function of time and frequency. The results are shown in Figure 5. One can see that the start and the end of the ship noise blocks were well resolved (panels A and B; see panel C for the spectrogram) at all occasions except the change from the ship noise to Gaussian noise (at 32 s) when only a single transient was detected since the transition period was too short. The panels D and E are given for reference. They demonstrate that while the respective transient changes had been resolved by the first two statistical moments as well, the relative TFC gradients were not so well pronounced as compared to r^2, and the definition of a threshold for a transient detection would have been less straightforward. While the presented simplified example is useful in terms of understanding of transient detection basics based on the present approach, more realistic examples are required to show its usefulness. This is done in the next section.

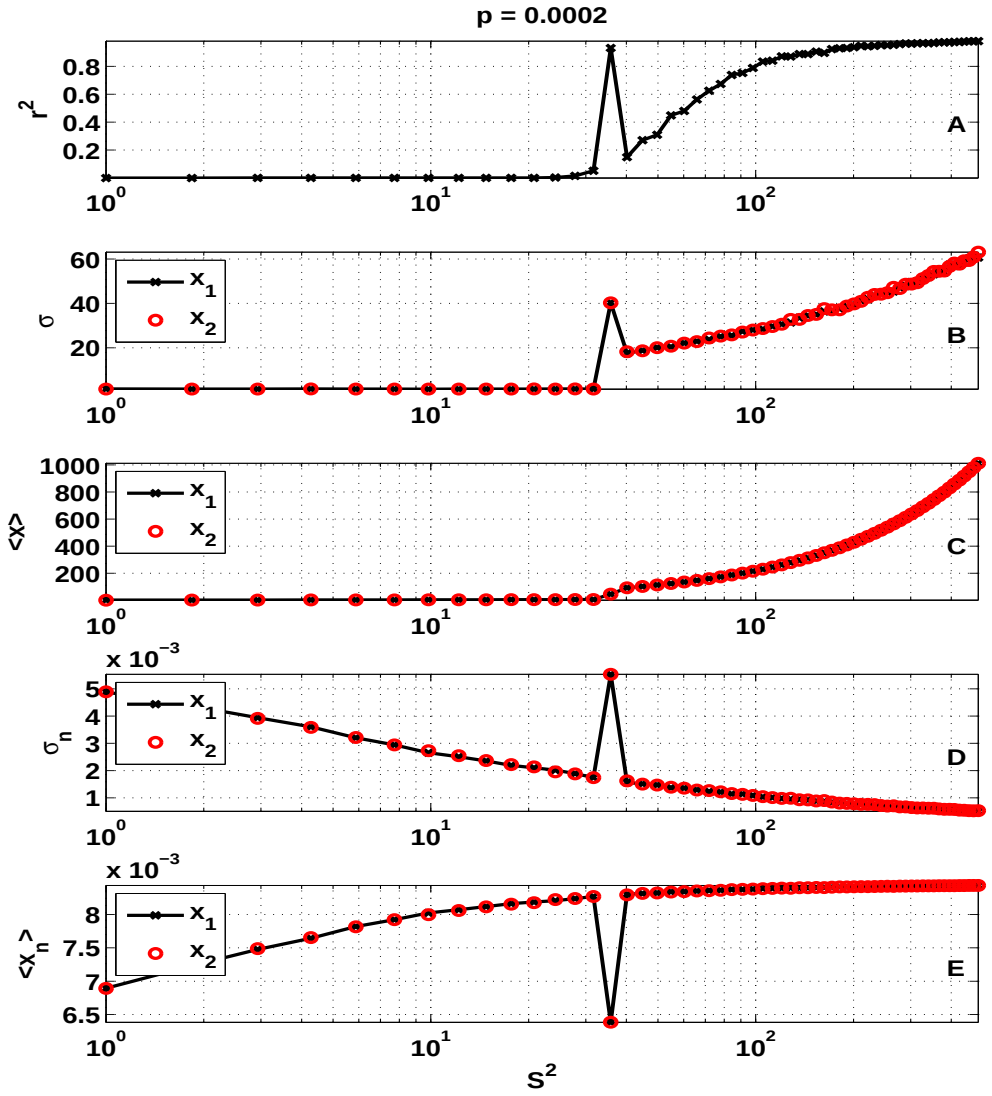

Figure 2: *Simulated change of: (A)- correlation between the pairs of centres of masses of TF cells in a feature space (eq. 7), (B, C)- the first two statistical moments of TF cells (equations 9, 10, 11), and (D,E)- the first two statistical moments of normalized (equation 8) TF cells as a function of* s_i^2 *(equation 12)*

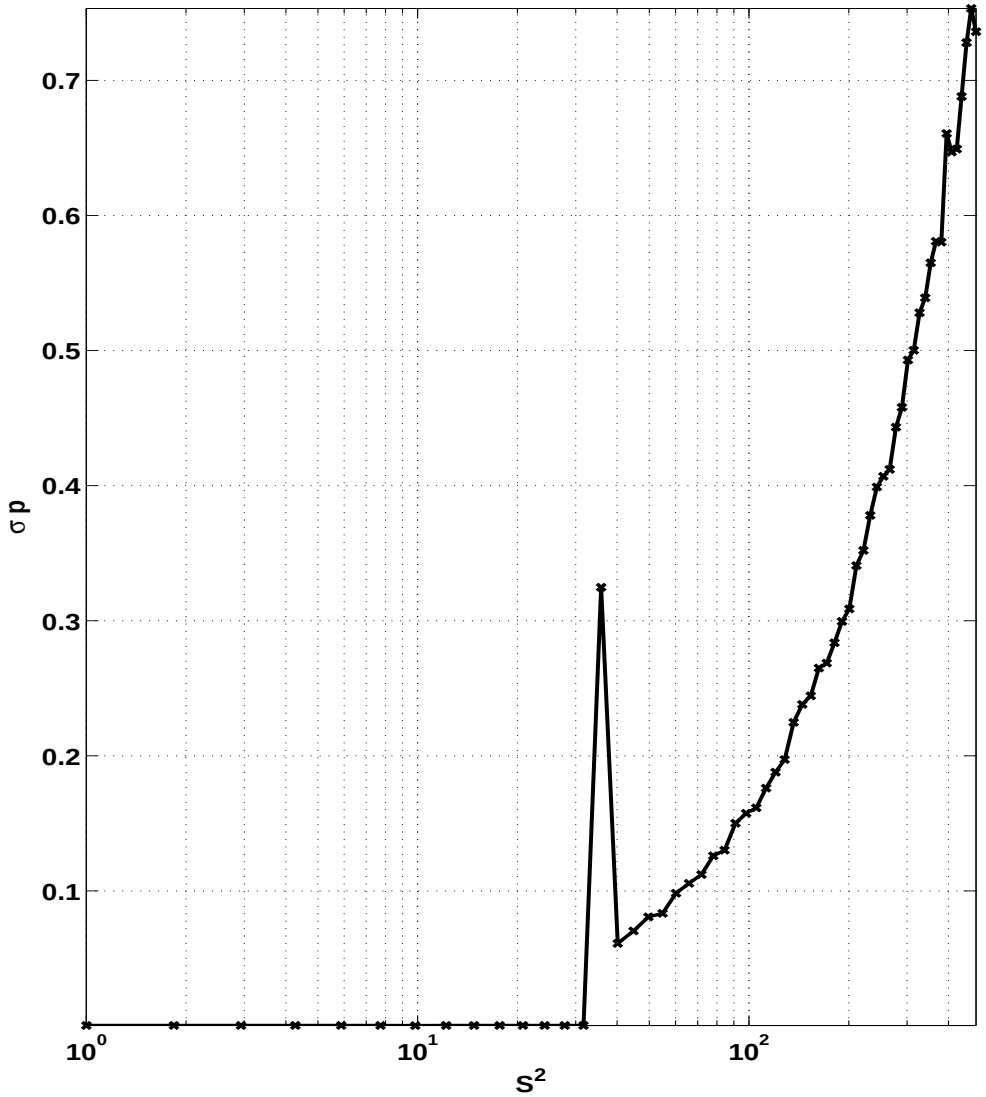

Figure 3: *Distribution of $p\sigma$ as a function of s_i^2*

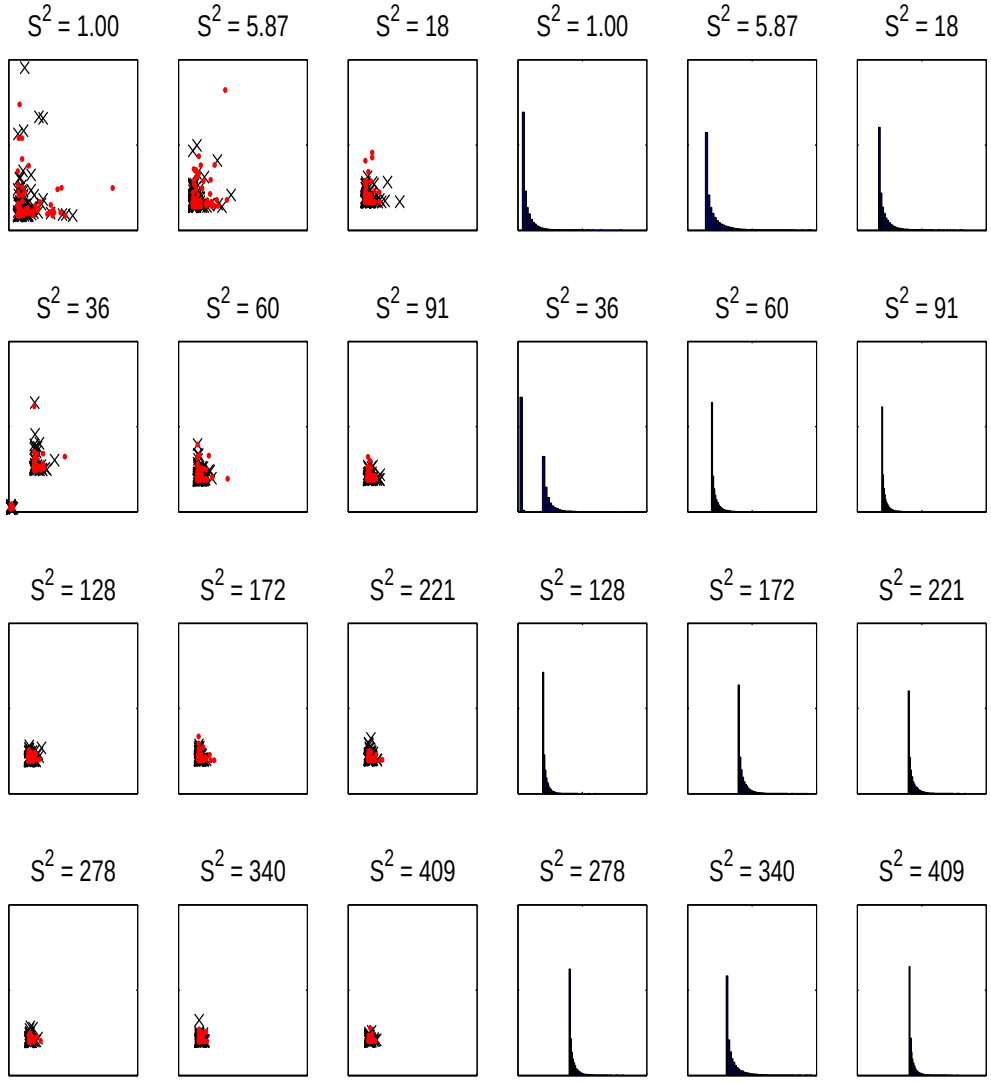

Figure 4: *Three leftmost columns: distribution of two runs (the different runs are shown by the different colors) of simulated data shown along the first two dimensions; three rightmost columns: histograms of two simulated data sets combined* $\mathbf{X_{i,1}}, \mathbf{X_{i,2}}$. *Note that a transient occurs at* $s_i^2 = 36$

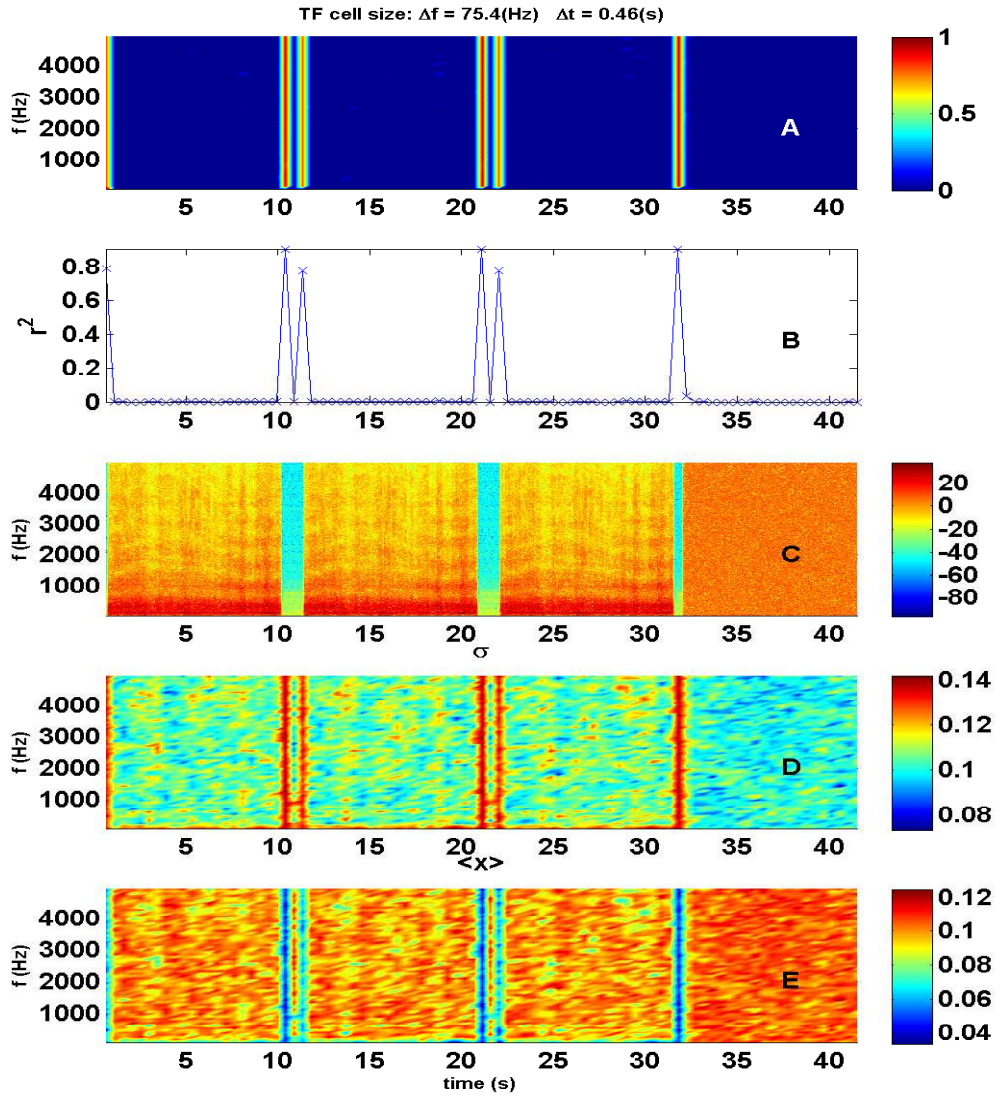

Figure 5: *Results of transient detection from the artificially generated onsets and stops of a ship engine. The same recording was used repeatedly three times (the first three blocks) followed by the appended Gaussian noise at the end (the fourth block). A- distribution of* r^2 *as a function of time and frequency; B- distribution of mean* $r^2 > 0.001$ *estimated for all columns of data shown in panel A; C- spectrogram of concatenated ship noise; D - distribution of standard deviation of normalized TF cells; E - distribution of mean values of normalized TF cells*

3 Results of Detection of Transients

The results presented in this section are based on the data sources open to public at the World Wide Web sites [7, 8]. The time series of acoustical data were extracted from WAV files (in a case of other formats, the respective files were first converted to WAV files), and divided into data sets each 1024 data points long. At the sampling frequency of $Fs =$ 11025 Hz, the frequency resolution was 10.8 Hz, and the upper frequency limit set to 5500 Hz. Inspection of Figures 6-11 shows that the proposed method detects well the

Data Description	Freq. Limits (Hz)	Transients	Fig. No
Live torpedo shot taken aboard an American submarine	0-5000	Torpedo launch at 1 s; hatch closing at 11 s, explosion at 30 s	6
Ship noise	0 - 5000	No detected transients	7
Motor boat	0 - 5000	Start of the engine (0.5 s), engine shifting into gear (8.5 s), stop of the engine (15.5 s)	8
Motor boat	0 - 5000	No detected transients	9
Pings of active sonar	100 - 2000	Onset and end of pings is resolved to limited extent	10
Live torpedo shot taken aboard an American submarine	1200 - 1600	decreasing the bandwidth as compared to the first row of this table improves visibility of the BB transient due to hatch closure but does not affect the respective mean value of r^2	11

Table 1: *Table of acoustical files analyzed in terms of detection of BB transients*

broadband transients and is insensitive to other types of spectral changes observed in the spectrograms. It can be especially well seen in the panels of two-dimensional distribution of r^2. A one-dimensional novelty index was based on the mean of $r^2 > 0.001$ estimated at each TFC time-instant. Looking at the spectrogram of Figure 6 one can notice two well pronounced broadband changes in spectral energy: the first during the torpedo launch, and the second during the explosion. The hatch closing was slightly better pronounced in the lower frequencies (up 2800 Hz) and generally was not resolved well at the given TFC resolution. Consequently the mean r^2 values appeared to be lower as compared to other transients respectively. Inspection of the spectrograms in the Figures 7, 9 shows no BB

transients. This corresponds well to the values of the estimated r^2, which were low during the whole time of observations.

If some a priori information were available about the frequency band of interest it could be used to filter out the transients observed out-of band of interest. Such an example is given in Figure 11. In this case by limiting the bandwidth to 1200-1600 Hz, one can observe more clearly a transient related to the hatch closure at 11 s and suppress some variability observed around 2000 Hz prior to the torpedo explosion. Finally, it must be noted that the choice of the size of a TF cell must be based on some preliminary experiments with the spectrograms of real life measurements. However, the tests with a wide range of different scenarios shown in this work show that once a respective size of TFC has been established, it can be used during a number of experiments unchanged (given that the sampling frequency remains constant).

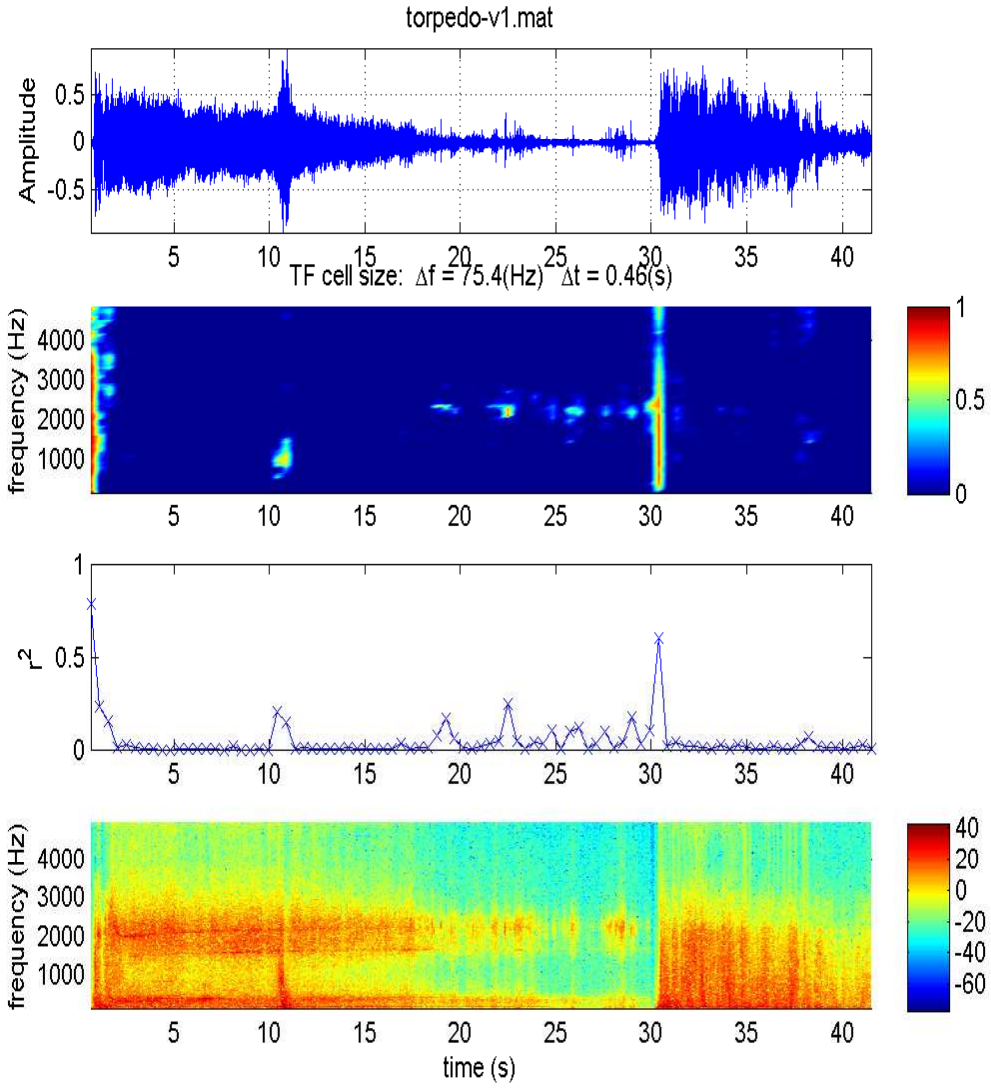

Figure 6: *Detection of the transients related to a torpedo launch (1 s), hatch closing (11 s) and explosion (31 s). The top panel- time series of recorded data; the second panel from the top- distribution of r^2 as a function of time and frequency; the third panel from the top- distribution of mean $r^2 > 0.001$ estimated for all columns of data shown in the second panel; the bottom panel-spectrogram of data shown in the top panel*

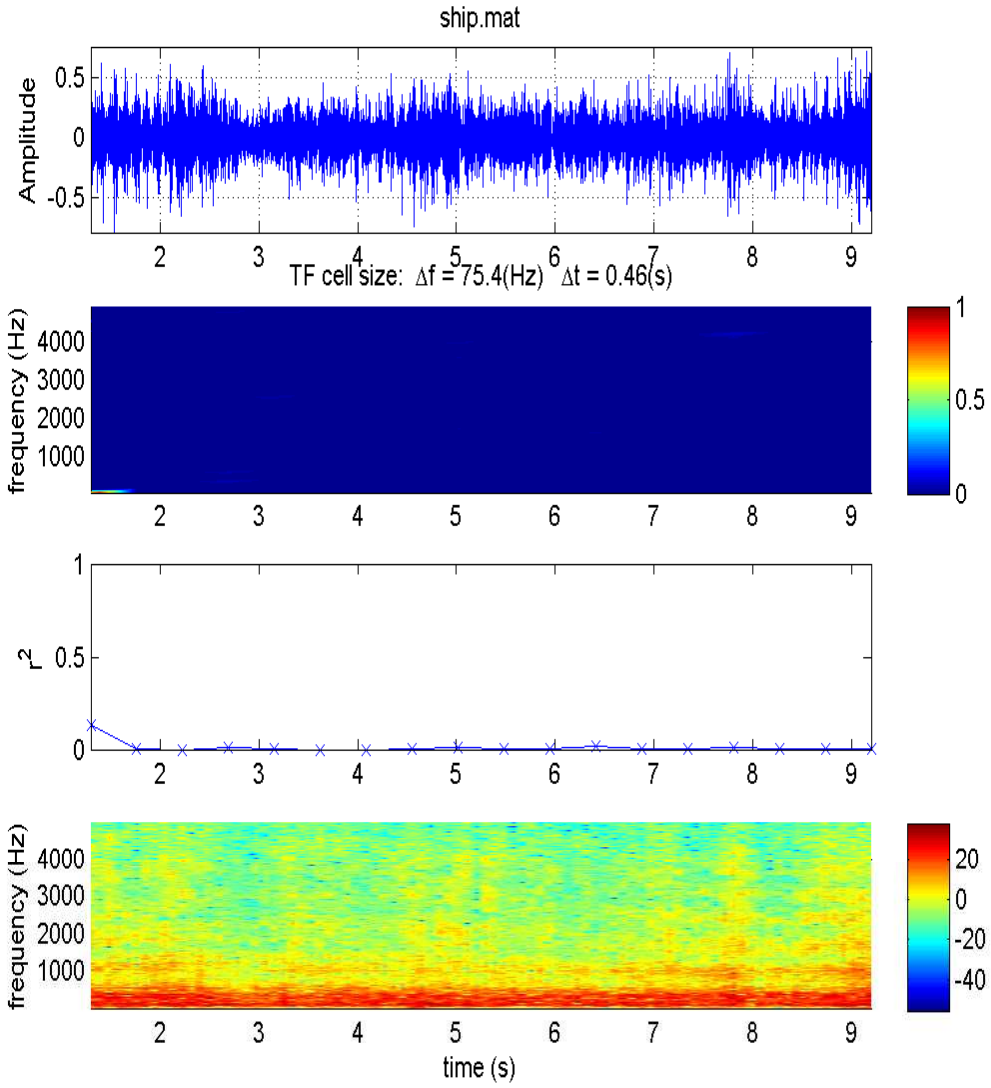

Figure 7: *Detection of the transients related to a ship engine noise. No visible BB transients can be noted (bottom panel). The top panel- time series of recorded data; the second panel from the top- distribution of r^2 as a function of time and frequency; the third panel from the top- distribution of mean $r^2 > 0.001$ estimated for all columns of data shown in the second panel; the bottom panel-spectrogram of data shown in the top panel*

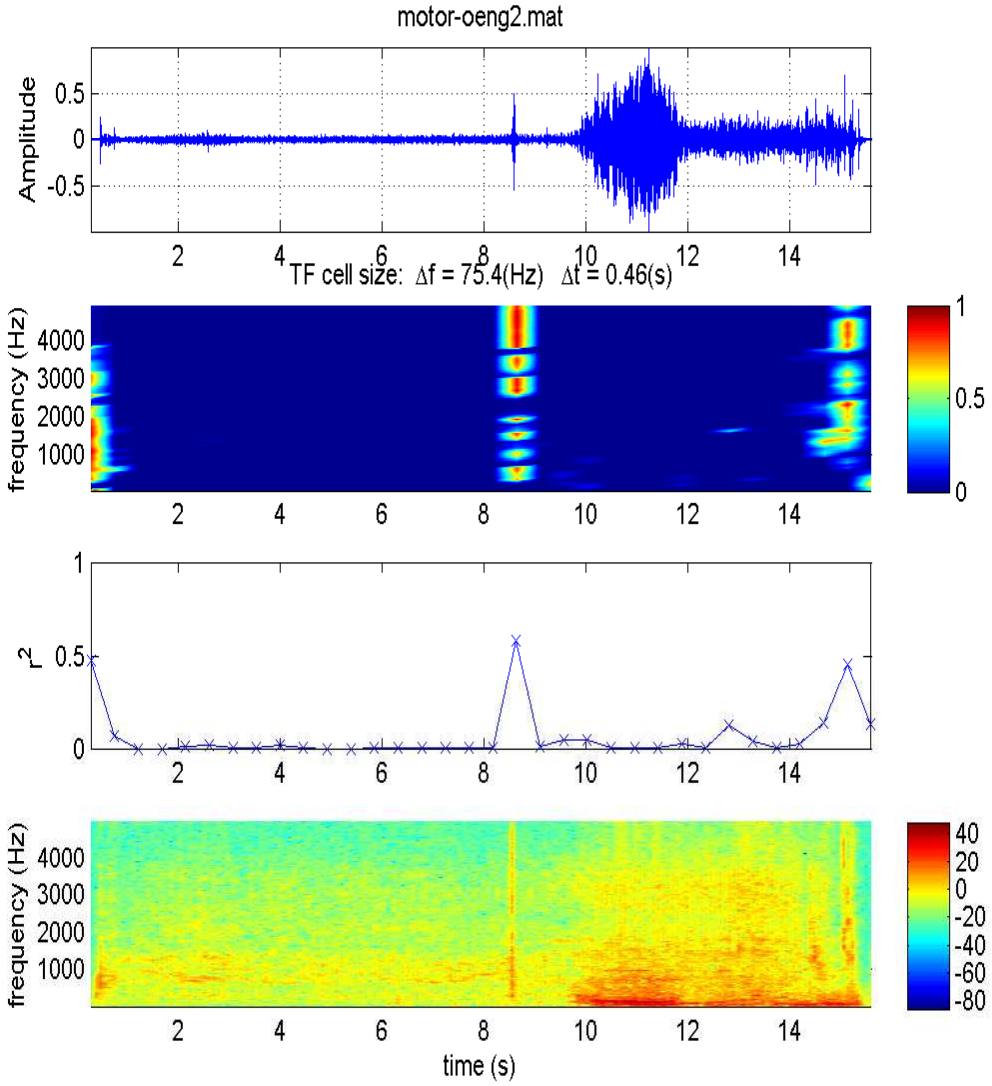

Figure 8: *Detection of the transients (1 s- start of the engine, 8.5 s - engine shifting into gear, 14.8 s - stop of the engine) related to a first motor-boat. The top panel- time series of recorded data; the second panel from the top- distribution of r^2 as a function of time and frequency; the third panel from the top- distribution of mean $r^2 > 0.001$ estimated for all columns of data shown in the second panel; the bottom panel-spectrogram of data shown in the top panel*

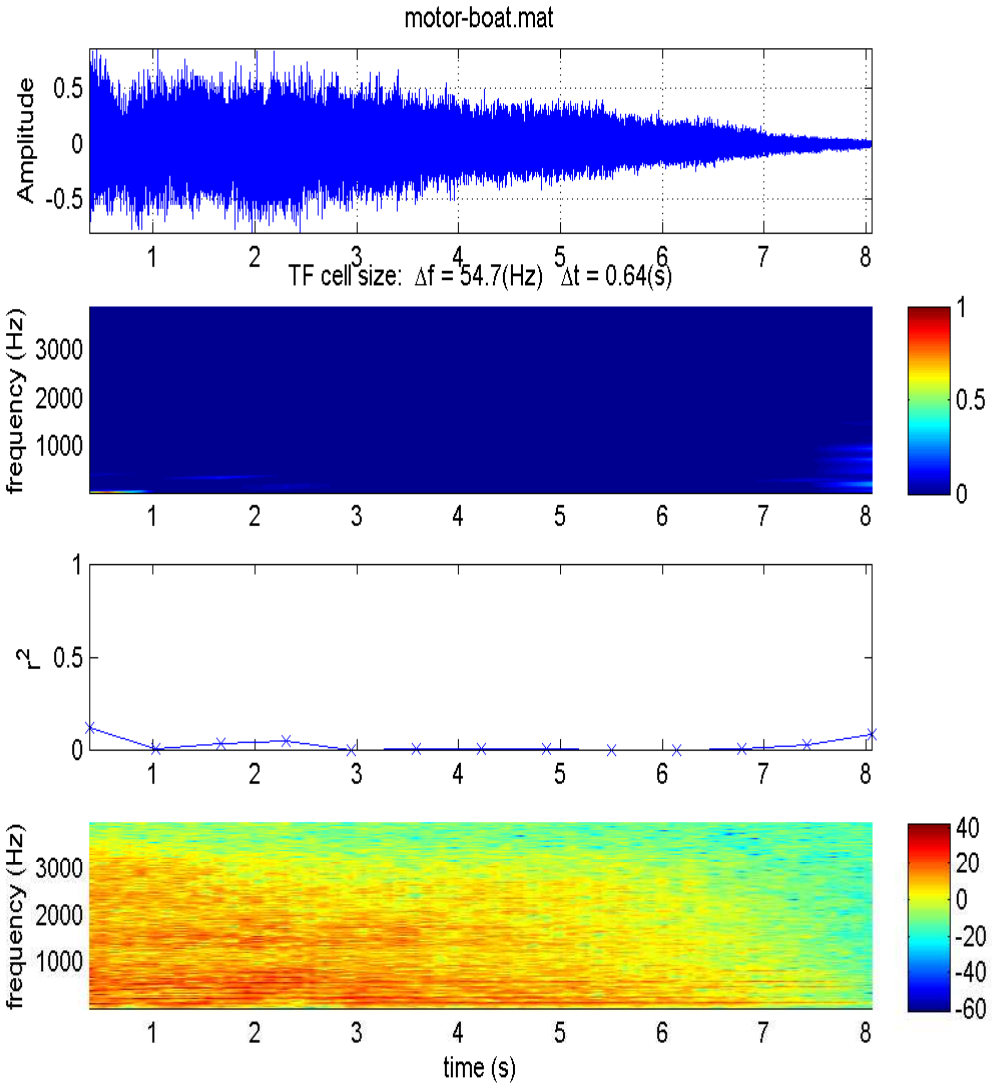

Figure 9: *Detection of the transients related to a second motor-boat. No visible transients can be observed. The top panel- time series of recorded data; the second panel from the top- distribution of* r^2 *as a function of time and frequency; the third panel from the top- distribution of mean* $r^2 > 0.001$ *estimated for all columns of data shown in the second panel; the bottom panel-spectrogram of data shown in the top panel*

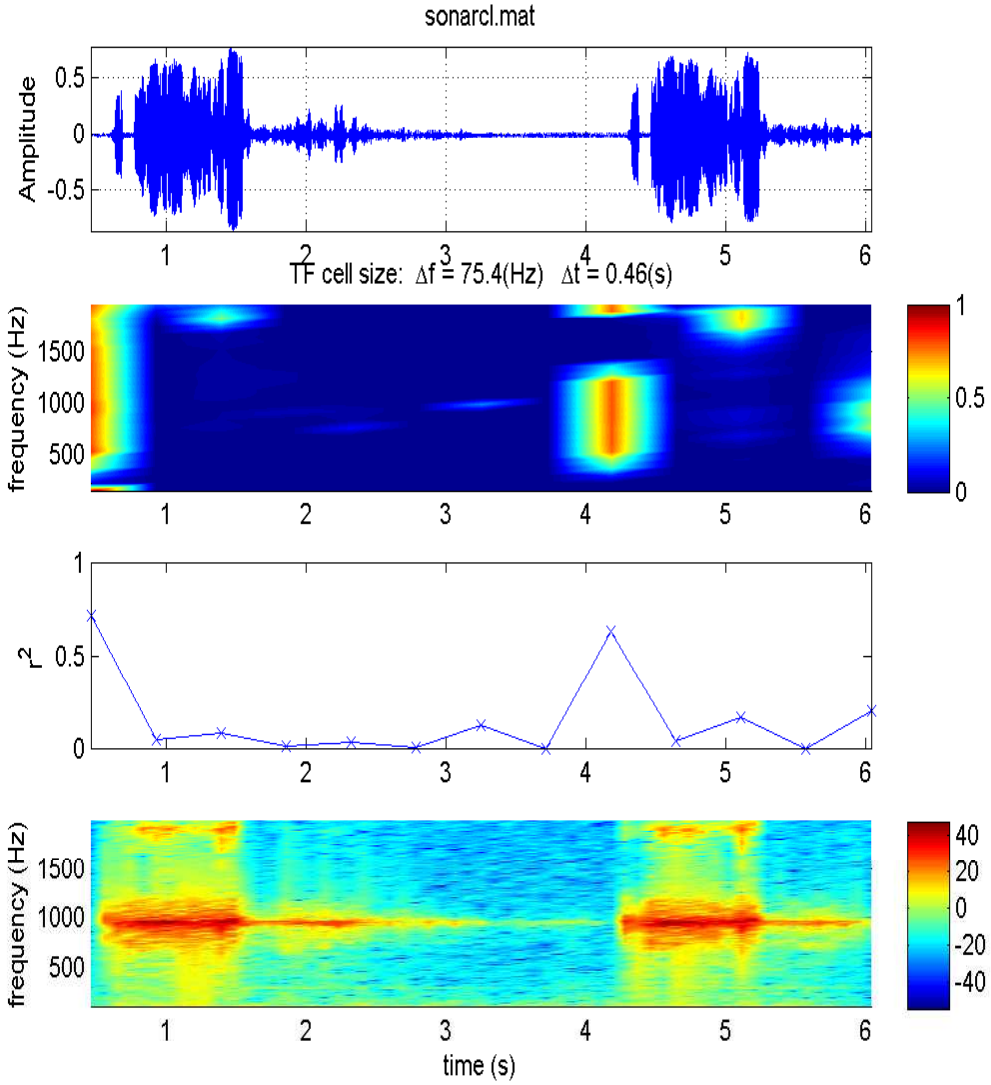

Figure 10: *Example of an active sonar signal; The top panel- time series of recorded data; the second panel from the top- distribution of* r^2 *as a function of time and frequency; the third panel from the top- distribution of mean* $r^2 > 0.001$ *estimated for all columns of data shown in the second panel; the bottom panel-spectrogram of data shown in the top panel*

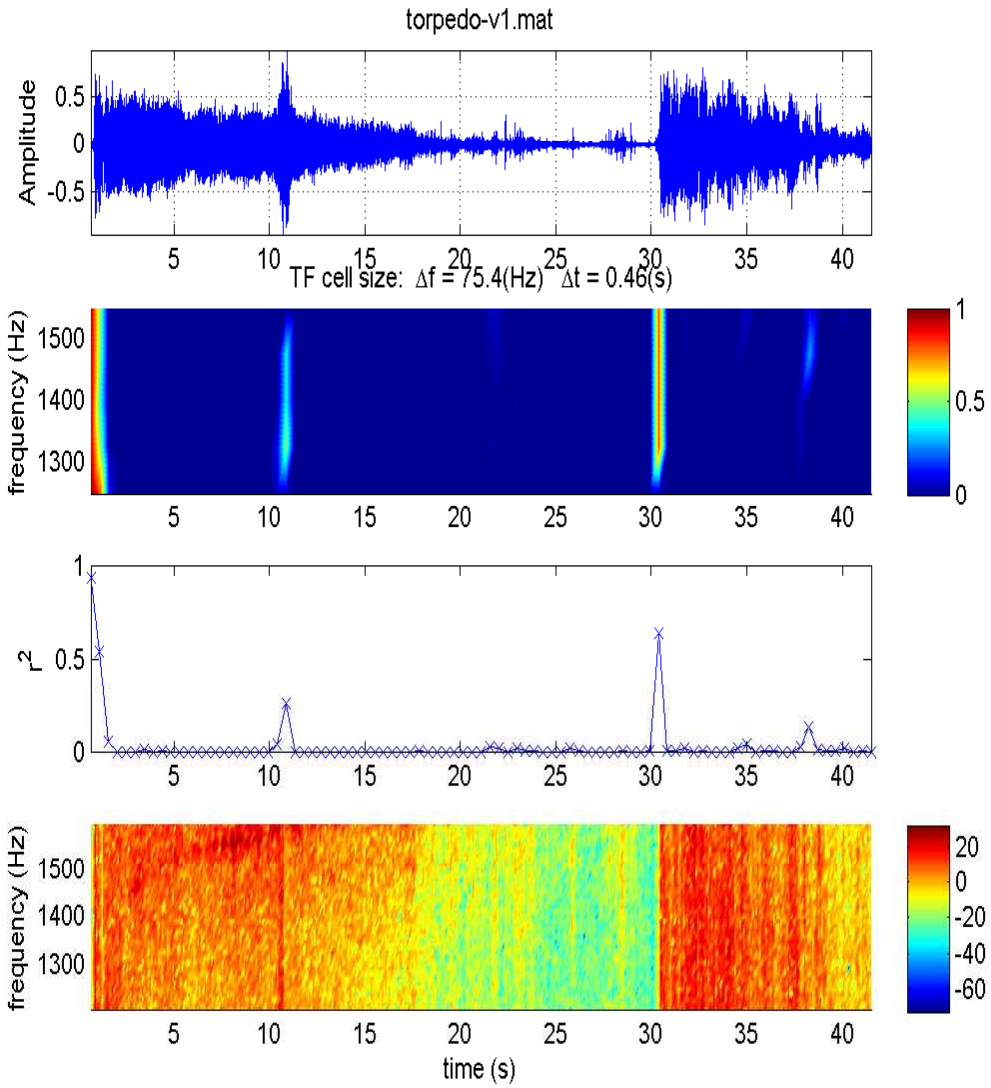

Figure 11: *The same as in Figure 6 with the only difference that in the present case data was analyzed for the bandwith 1200-1600 Hz*

4 Transient Detection in Beamformed Data

In the context of Naval acoustic applications, one of the approaches of transient detection is based on hydrophones measurements arranged in towed arrays. In a case of known array shape, the simultaneous measurements improve signal to noise ratio as well as provide information about bearings of spatially localized acoustical sources. However, array shape estimation can sometimes be a difficult problem (e.g. during turns). Errors in array shape estimation lead to degradation of information extracted from data. Therefore it will be interesting to test performance of BB transient detection under different error conditions. To do this we will use two data sets analyzed in the previous section: torpedo launch-target hit and ship noise records. Since the ship noise record was shorter, we will increase ship noise record to the length of torpedo record by using the same ship noise measurements three times (by concatenating them together), plus extending the concatenated measurements by zeros to match the length of torpedo record. Assuming that during the whole period of measurements the torpedo and the ship were located in the far-field at distinctly different constant bearings θ_1 and θ_2 at equal distance from the array, the following array spectral matrix at frequencies $\mathbf{f}$ and at array elements $\mathbf{n}$ would have been obtained:

$$\mathbf{X}(f,n) = 0.5\left(\mathbf{x_1}(f)e^{i2\pi f(z_n sin(\theta_1) - y_n cos(\theta_1))/c} + \mathbf{x_2}(f)e^{i2\pi f(z_n sin(\theta_2) - y_n cos(\theta_2))/c}\right) \quad (14)$$

where c is sound speed, $\mathbf{x_1}(\mathbf{f})$ and $\mathbf{x_2}(\mathbf{f})$ are complex spectra of torpedo and ship respectively, z_n and y_n relative horizontal coordinates of array elements. Assuming that the array shape, the bearings of the torpedo and ship were known, conventional beamforming was performed at the bearings $\theta = \theta_1$ and $\theta = \theta_2$.

$$\hat{\mathbf{X}}(f) = \Sigma_n \mathbf{X}(f,n)e^{-i2\pi f(z_n sin(\theta) - y_n cos(\theta))/c} \quad (15)$$

From results of transient detection given in the Figures 12, 13 one can see that the obtained results of the distribution r^2 were essentially same as in a case of analysis of original time series (Figures 5, 6). Next, we used an incorrect array shape (y_n was set to 0 and $z_n = nd$, where d was a constant distance between array elements). Thus, beamforming was carried out using

$$\hat{\mathbf{X}}(f) = \Sigma_n \mathbf{X}(f,n)e^{-i2\pi f n d sin(\theta)/c} \quad (16)$$

The respective results are shown in Figure (14). The transients due to the launch of torpedo and the target hit were still detectable. Finally, additionally to the wrong array shape, a torpedo bearing error of 20 degrees ($\theta = \theta_1 + 20$) was introduced (equation (16)). Although, in this case r^2 was reduced, the two transients were still observable. Finally, as a quality check of the performed calculations, the array shape was estimated using eigenvector method ([10]) using only acoustical data (equation (14)), known torpedo bearing θ_1, and distance between array elements. Figure 16 shows that the array shape was estimated accurately.

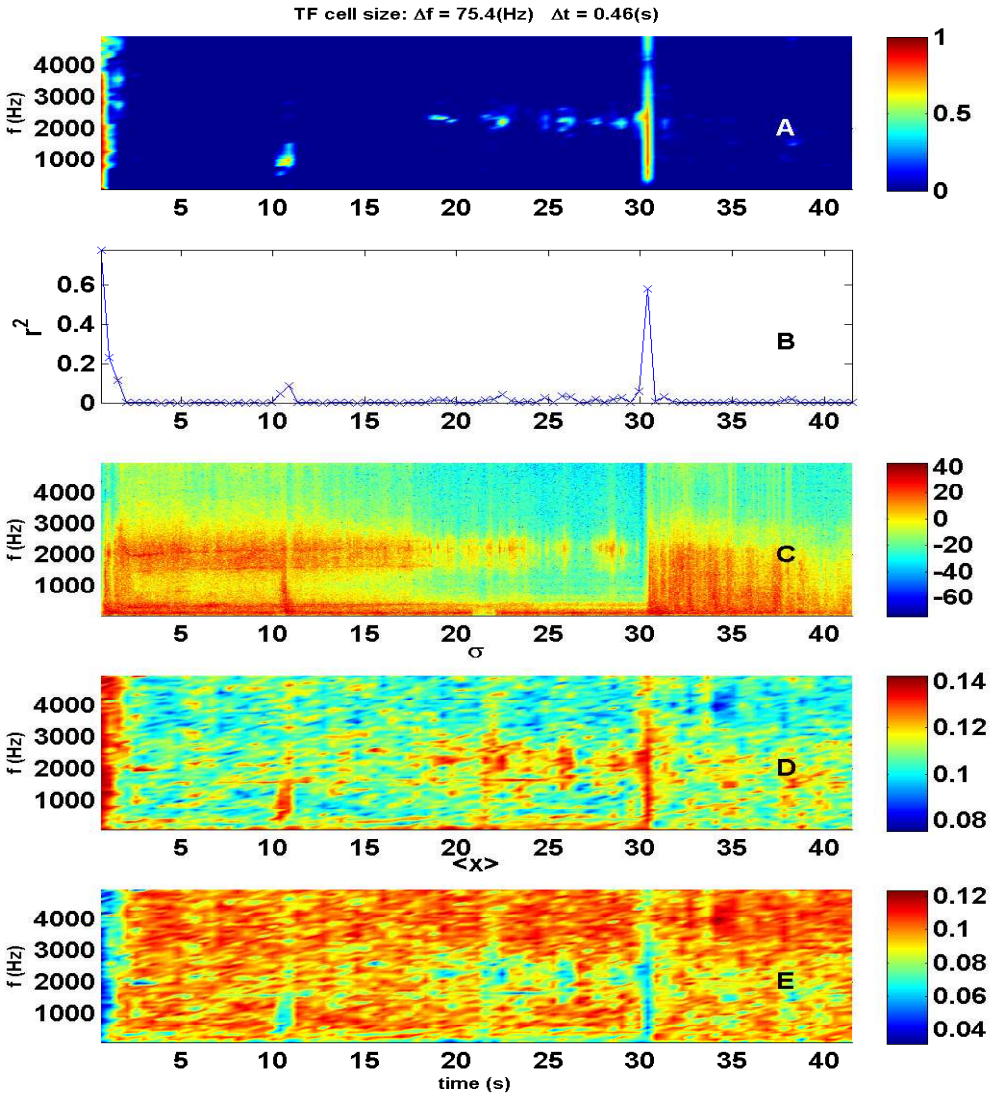

Figure 12: *Detection of transients based on beamformed data with a look at a torpedo bearing; A- distribution of r^2 as a function of time and frequency; B- distribution of mean $r^2 > 0.001$ estimated for all columns of data shown in panel A; C- spectrogram of concatenated ship noise; D - distribution of standard deviation of normalized TF cells; E - distribution of mean values of normalized TF cells*

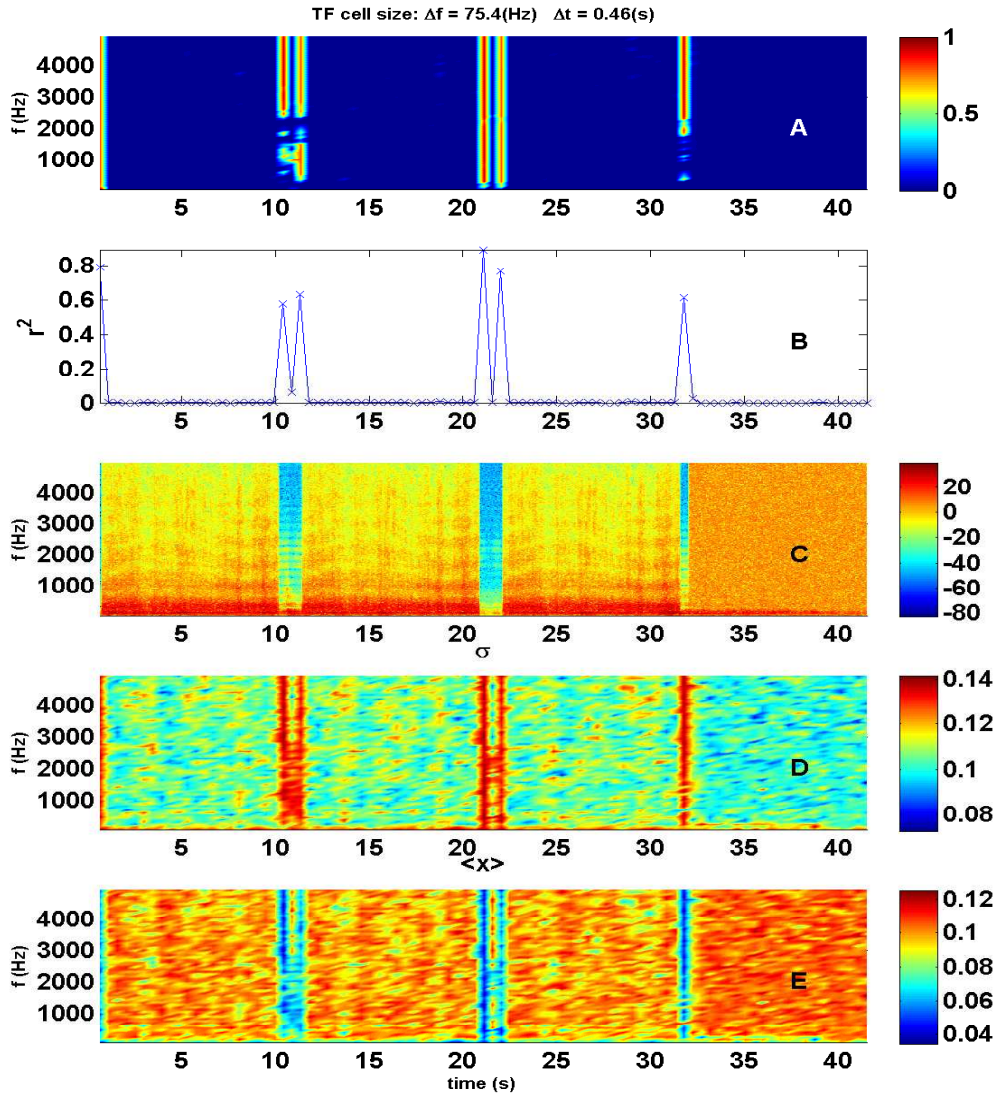

Figure 13: *Detection of transients based on beamformed data with a look at the ship bearing; A- distribution of r^2 as a function of time and frequency; B- distribution of mean $r^2 > 0.001$ estimated for all columns of data shown in panel A; C- spectrogram of concatenated ship noise; D - distribution of standard deviation of normalized TF cells; E - distribution of mean values of normalized TF cells*

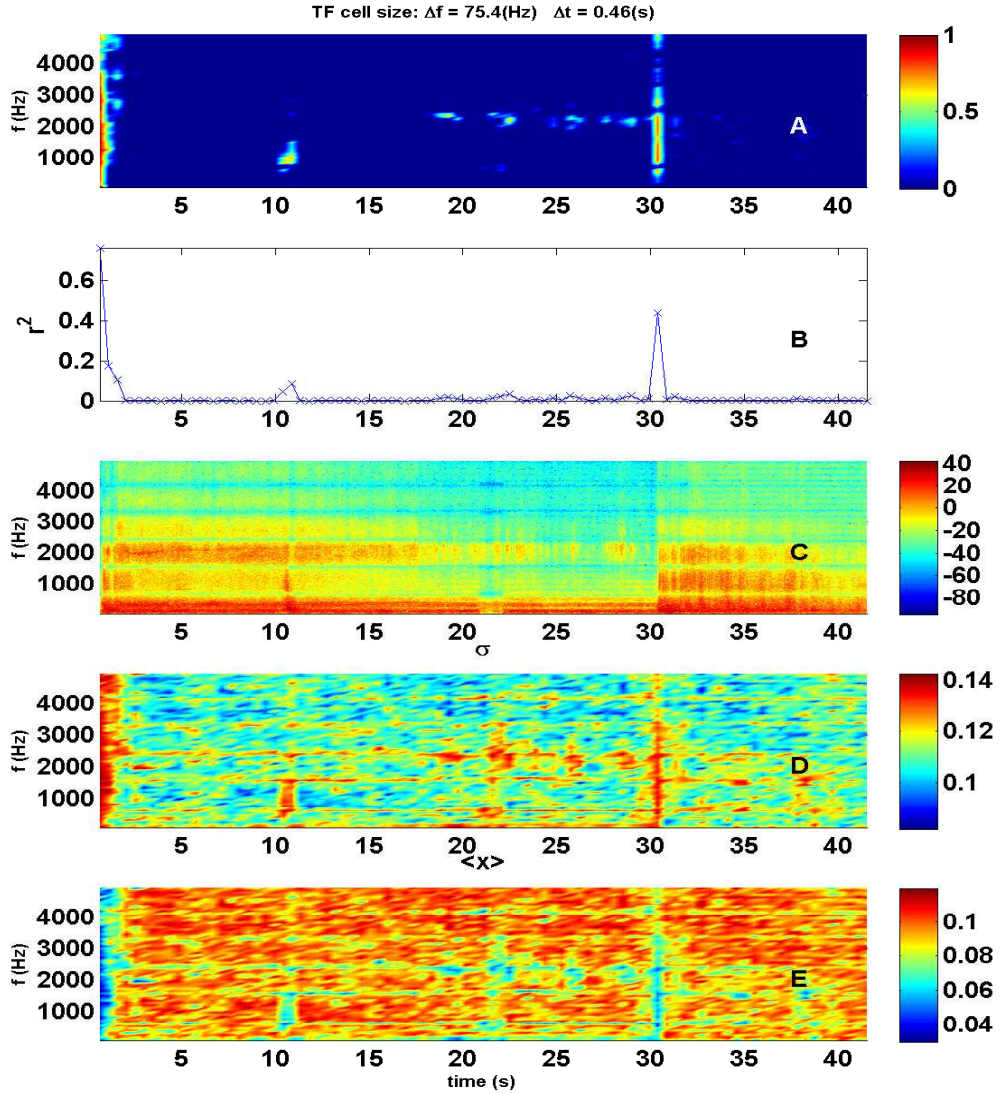

Figure 14: *Detection of transients based on beamformed data using incorrect array shape with a look at the torpedo bearing; A- distribution of r^2 as a function of time and frequency; B- distribution of mean $r^2 > 0.001$ estimated for all columns of data shown in panel A; C- spectrogram of concatenated ship noise; D - distribution of standard deviation of normalized TF cells; E - distribution of mean values of normalized TF cells*

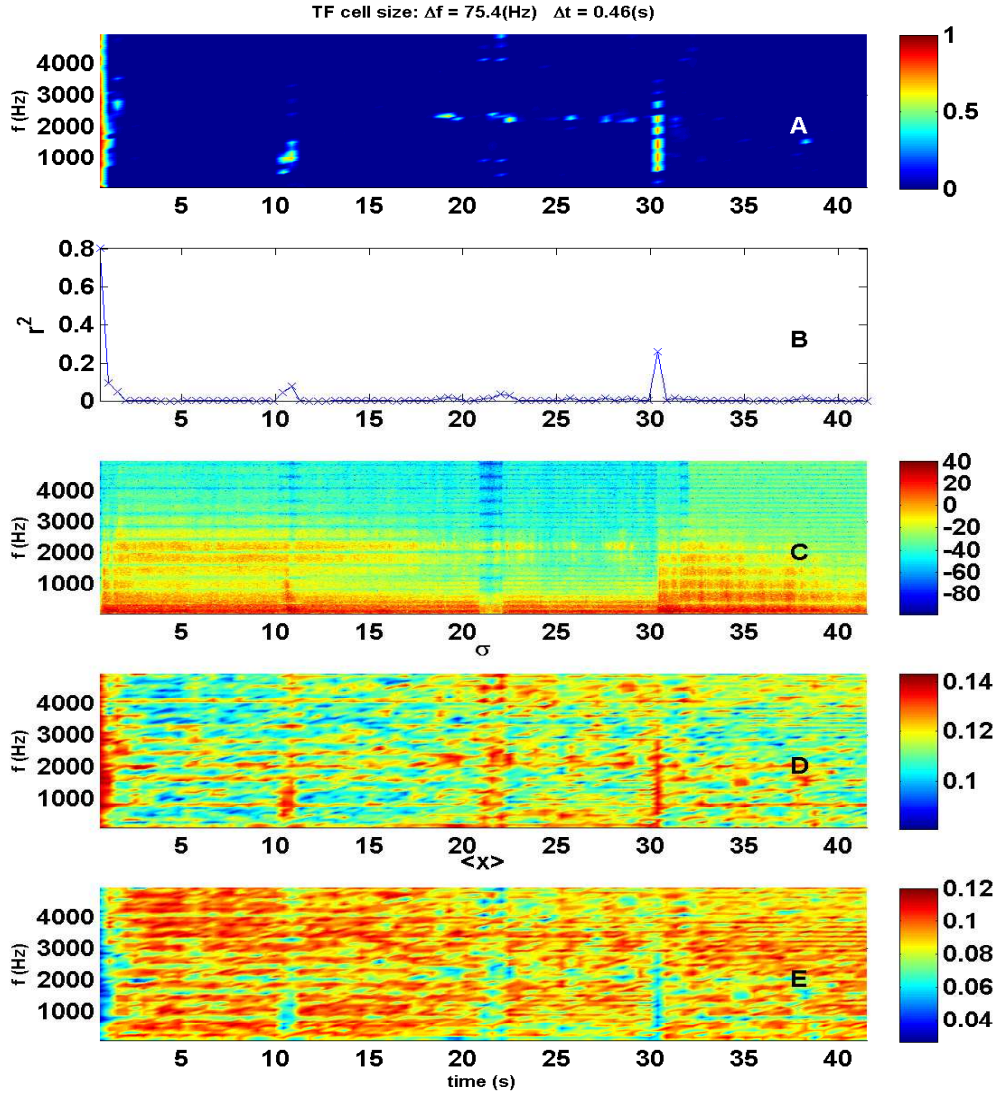

Figure 15: *Detection of transients based on beamformed data using incorrect array shape and incorrect torpedo bearing of 20 degrees; A- distribution of r^2 as a function of time and frequency; B- distribution of mean $r^2 > 0.001$ estimated for all columns of data shown in panel A; C- spectrogram of concatenated ship noise; D - distribution of standard deviation of normalized TF cells; E - distribution of mean values of normalized TF cells*

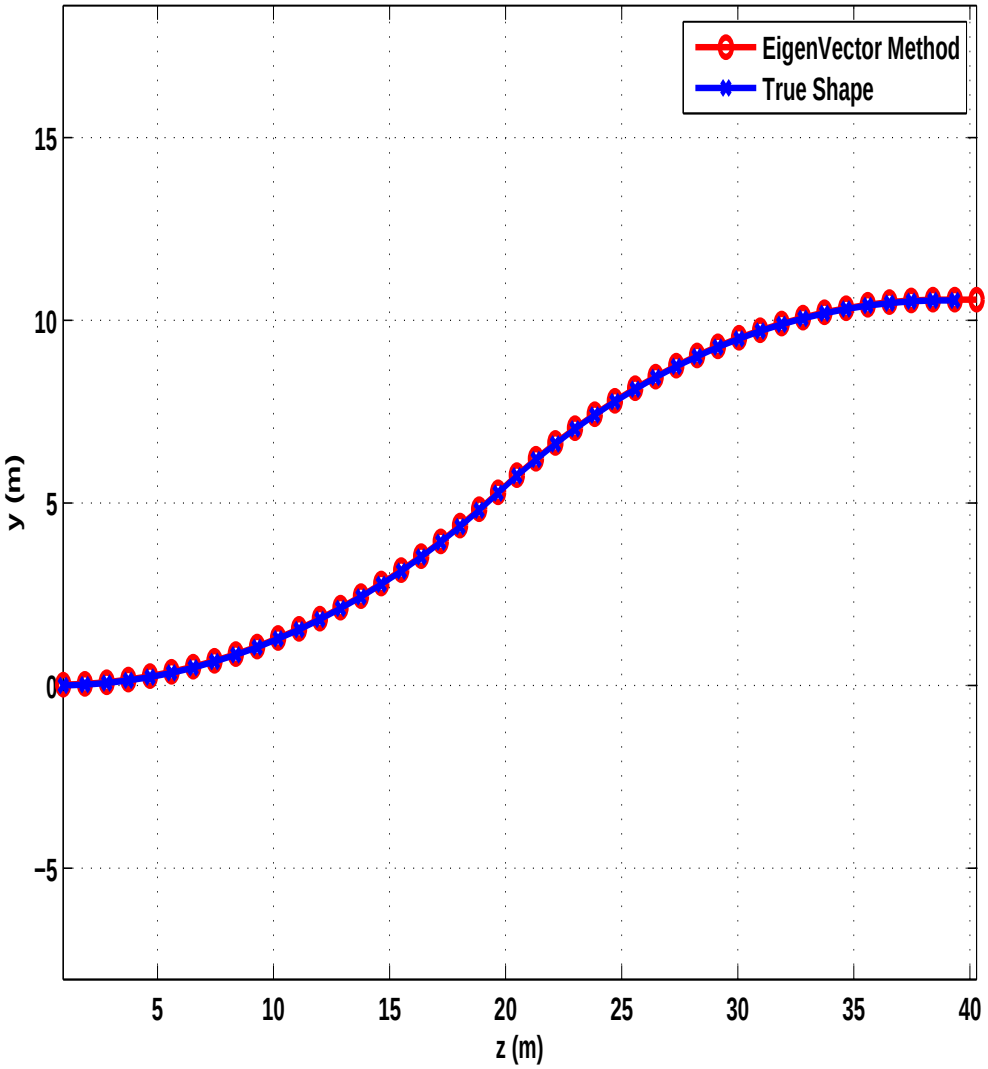

Figure 16: *Array Shape: true (blue) and estimated (red) from eigenvector method*

5 Discussion

In this work an $ad\ hoc$ approach has been proposed for detection of BB transients, which manifest themselves as a sudden increase in spectral energy observed over a short time in a broad band of frequencies. DBBT acts like a filter in a sense that if the variances of the respective normalized TFC are significantly lower as compared to the spread factor p of a Gaussian kernel, correlation of the centre of masses of TFCs in a feature space decreases significantly. Because of data normalization, carried already out in the input time-frequency space, one would expect that the proposed approach should be relatively robust to the changes in absolute energy levels of spectrograms. Of course, should the variance of normalized TF data be significantly higher than p, high correlation of the centre of masses of TFC in a feature could be observed regardless the existence of transients. Hence, the key to the successful application of DBBT is to have some a priori information about the variance values of normalized spectra of TFCs. The preliminary tests of DBBT have shown that this approach can be used without any changes of settings in a number of different measurement conditions.

One may be tempted to modify DBBT for detection of narrow-band signals or for changing the axis of similarity analysis from frequency to time. The results based on simulated data (Figures 17, 18) respectively show that the respective changes can be successful in a simulated environment. However, one may experience significant difficulties in obtaining a robust algorithm for the respective real-world problems. More real-life measurements are needed to see how successfully the modified DBBT can be applied. Finally, it would be interesting to test the proposed algorithm on data from Halifax-class towed, hull-mounted sonars and sono-buoys from recent torpedo exercises. The preliminary results obtained in this work indicate that DBBT should show good results in terms of false alarms and it should work well with the BB transients observed in the time intervals comparable to a TF cell size.

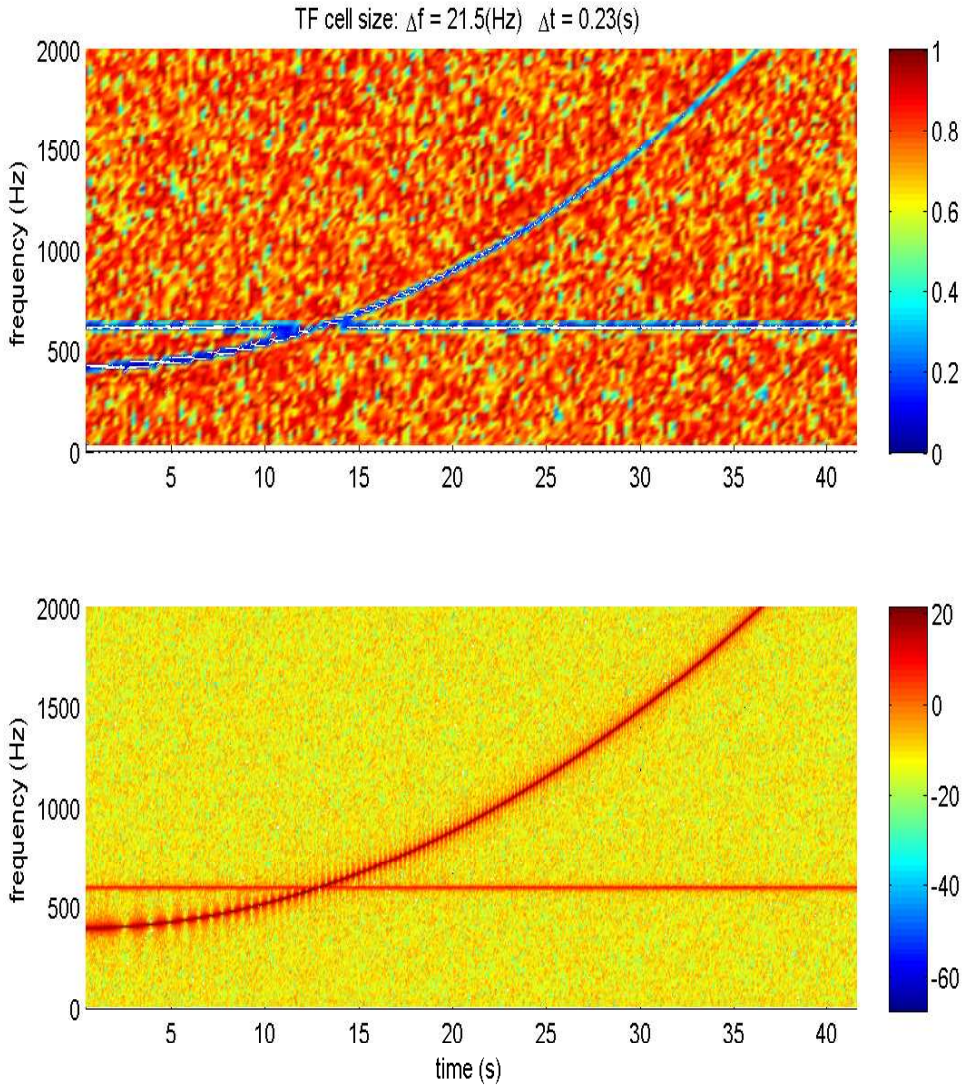

Figure 17: *Quadratic frequency modulated chirp and a tonal mixed with white Gaussian noise. Upper panel: distribution of r^2 as a function of time and frequency. Gaussian spread parameter is set such that background noise appears to be correlated in a feature space whereas the detected signals exhibit r^2 close to zero. Lower panel: spectrogram of given data*

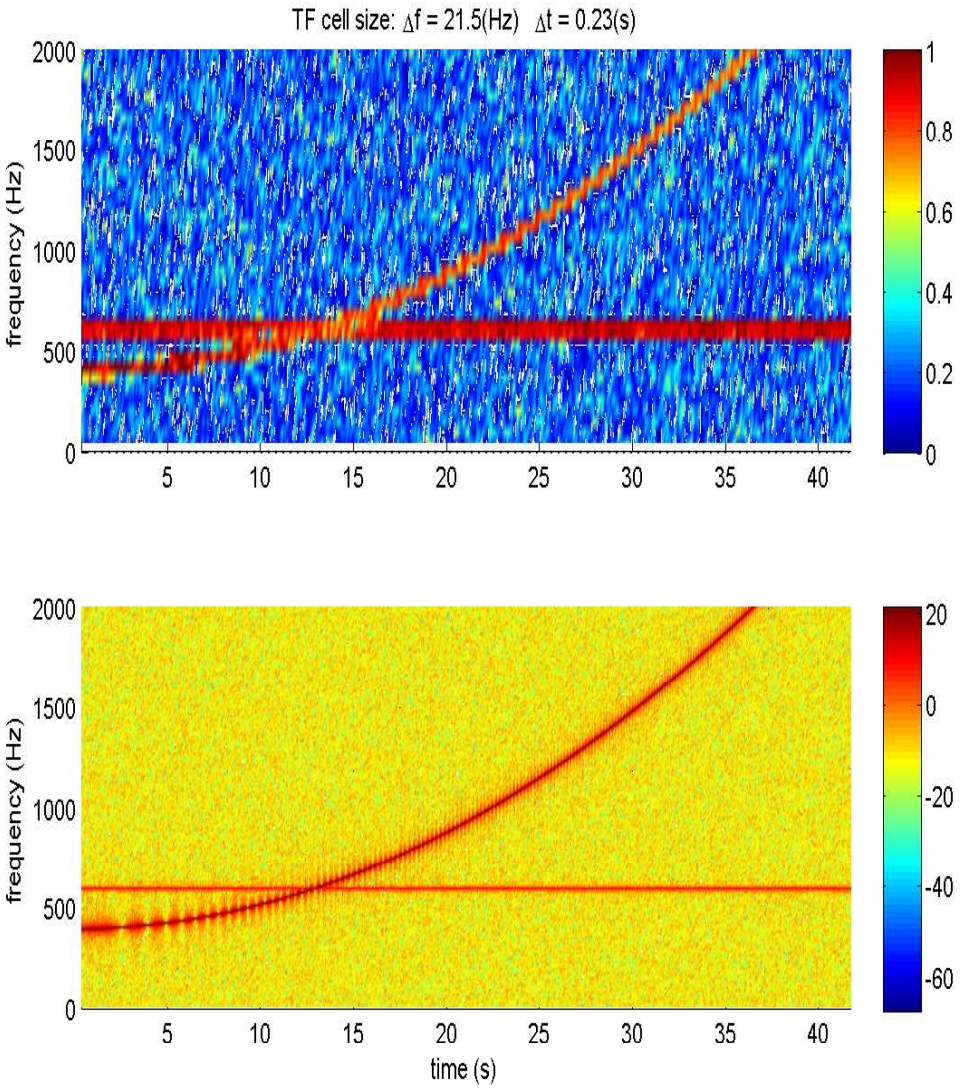

Figure 18: *Quadratic frequency modulated chirp and a tonal mixed with white Gaussian noise. Upper panel: distribution of r^2 as a function of time and frequency. Similarity analysis is carried out along time axis (whereas in the upper Figure, as well as in the rest of this work it is carried out along frequency axis) Gaussian spread parameter is set such that background noise appears to be uncorrelated in a feature space whereas the detected signals exhibit r^2 close to one. Lower panel: spectrogram of given data*

6 Conclusions

In this work a novel approach for detection of broadband transients has been proposed. DBBT was able to detect the transients that manifest themselves as a sudden increase in spectral energy observed in a short time over a broad band of frequencies. In contrast to the approaches of transient detection, which *directly* test the signal changes in time, DBBT tests for similarity of time-frequency cells along a frequency axis to decide whether there were any significant changes in time. Preliminary tests of BB transient detection, carried out using a number of real-world data sets, demonstrate robustness of the proposed method.

References

[1] Han, C., P., Willett, B., Chen, and D., Abraham (1998), A Detection Optimal Min-Max Test for Transient Signals, *IEEE Transactions on Information Theory*, 44(2), 866–869.

[2] Abraham, D. A. and P.K., Willet (2002), Active Sonar Detection in Shallow Water Using the Page Test, *IEEE Journal of Oceanic Engineering*, 27(1), 35–46.

[3] Hory, C., Martin, N., and A., Chehikian (2002), Spectrogram Segmentation by Means of Statistical Features for Non-Stationary Signal Interpretation, *IEEE Transactions On Signal Processing*, 50(12), 2915–2925.

[4] Ginolhac, G., Chanussot, J., and Hory, C. (2005), Morphological and Statistical Approaches to Improve Detection in the Presence of Reverberation, *IEEE of Oceanic Engineering*, 30(4), 881–899.

[5] Desobry, F., Davy, M., and Doncarli, C. (2005), An online kernel change detection algorithm, *Signal Processing, IEEE Transactions on*, 53, 2961–2974.

[6] Sildam, J. (2006), A Preliminary Investigation of Support Vector Machines for Detection of Novel Targets, *DRDC-Atlantic Technical Memorandum TM 2006-270*.

[7] www.dosits.org/gallery/intro.htm.

[8] www.geocities.com/CapeCanaveral/1046/audio1.html.

[9] Shawe-Taylor, John and Cristianini, Nello (2004), Kernel Methods for Pattern Analysis, Cambridge University Press.

[10] Ferguson, Brian G. (1993), Remedying the Effects of Array Shape Distortion on the Spatial Filtering of Acoustic Data from a Line Array of Hydrophones, *IEEE Journal of Oceanic Engineering*, 18(4), 565–571.

This page intentionally left blank.

Distribution list

DRDC Atlantic TM 2006-258

Internal distribution

1 Mark Trevorrow, GL/TorD

1 Art Collier

1 John Fawcett

1 David Hopkin, GL/UFP

2 Juri Sildam, (1 CD, 1 hard copy)

1 David Hazen, H/TD

1 Nicole Collison

1 James Theriault

1 Sean Pecknold

1 Erin MacNeil, PM/MSDCL

1 Garry Heard, GL/NetALS

5 Library

Total internal copies: 17

External distribution

1 Bruce Martin
11 Thornhill Drive, Suite 102
Dartmouth, NS B3B 1B9

Department of National Defence

1 NDHQ/DRDC/DRDKIM 3

1 Orest Bluy, DSTM 4

1 LCDR A.D. Penney, DMRS 5-2

1 CO, ADAC(A)

1 CO, ADAC(P)

Total external copies: 6

Total copies: 23

DOCUMENT CONTROL DATA

(Security classification of title, body of abstract and indexing annotation must be entered when document is classified)

1. ORIGINATOR (the name and address of the organization preparing the document. Organizations for whom the document was prepared, e.g. Centre sponsoring a contractor's report, or tasking agency, are entered in section 8.)

   Defence R&D Canada – Atlantic
   P.O. Box 1012, Dartmouth, Nova Scotia, Canada
   B2Y 3Z7

2. SECURITY CLASSIFICATION (overall security classification of the document including special warning terms if applicable).

   UNCLASSIFIED

3. TITLE (the complete document title as indicated on the title page. Its classification should be indicated by the appropriate abbreviation (S,C,R or U) in parentheses after the title).

   A Novel Detector of Broadband Transient Signals

4. AUTHORS (last name, first name, middle initial)

   Jüri Sildam,

5. DATE OF PUBLICATION (month and year of publication of document)	6a. NO. OF PAGES (total containing information. Include Annexes, Appendices, etc).	6b. NO. OF REFS (total cited in document)
November 2006	48	10

7. DESCRIPTIVE NOTES (the category of the document, e.g. technical report, technical note or memorandum. If appropriate, enter the type of report, e.g. interim, progress, summary, annual or final. Give the inclusive dates when a specific reporting period is covered).

   Technical Memorandum

8. SPONSORING ACTIVITY (the name of the department project office or laboratory sponsoring the research and development. Include address).

   Defence R&D Canada – Atlantic
   P.O. Box 1012, Dartmouth, Nova Scotia, Canada B2Y 3Z7

9a. PROJECT NO. (the applicable research and development project number under which the document was written. Specify whether project).	9b. GRANT OR CONTRACT NO. (if appropriate, the applicable number under which the document was written).
11cw02	

10a. ORIGINATOR'S DOCUMENT NUMBER (the official document number by which the document is identified by the originating activity. This number must be unique.)	10b. OTHER DOCUMENT NOs. (Any other numbers which may be assigned this document either by the originator or by the sponsor.)
DRDC Atlantic TM 2006-258	

11. DOCUMENT AVAILABILITY (any limitations on further dissemination of the document, other than those imposed by security classification)

   (X) Unlimited distribution
   ( ) Defence departments and defence contractors; further distribution only as approved
   ( ) Defence departments and Canadian defence contractors; further distribution only as approved
   ( ) Government departments and agencies; further distribution only as approved
   ( ) Defence departments; further distribution only as approved
   ( ) Other (please specify):

12. DOCUMENT ANNOUNCEMENT (any limitation to the bibliographic announcement of this document. This will normally correspond to the Document Availability (11). However, where further distribution beyond the audience specified in (11) is possible, a wider announcement audience may be selected).

13. ABSTRACT (a brief and factual summary of the document. It may also appear elsewhere in the body of the document itself. It is highly desirable that the abstract of classified documents be unclassified. Each paragraph of the abstract shall begin with an indication of the security classification of the information in the paragraph (unless the document itself is unclassified) represented as (S), (C), (R), or (U). It is not necessary to include here abstracts in both official languages unless the text is bilingual).

A novel approach for detection of broad-band (BB) transients (DBBT) is proposed. DBBT is based on an analysis of the spectrograms, calculated from time series of one or more hydrophones. A spectrogram is divided into locally normalized time-frequency cells (TFC). Two TFCs, which are measured at the same time but at different neighboring frequencies, are said to include a signature of a broad-band transient signal if their empirical centres of masses estimated in a higher-dimensional feature space using a Gaussian kernel exhibit correlation higher than a predefined threshold. A spread coefficient p of a Gaussian kernel is chosen so that the correlation between the pairs of centres of masses of TFCs that do not include transient signatures appear to be uncorrelated. Tests of BB transient detection, carried out using a number of real-world data sets, demonstrate robustness of the proposed method. In particular, DBBT was able to detect the launch and explosion of a torpedo, the start and stop of small boat engine, and other events. Reusable values of size of TF cells, a p value, and correlation threshold were used. The same settings were also successfully used with two sets of torpedo and ship measurements artificially combined at different bearings within a framework of simulated beam-forming. The results were found to be relatively insensitive to the array shape and target bearing errors. A few tests that were carried out on artificially generated narrowband signals using modified DBBT were found to be too limited and therefore inconclusive.

14. KEYWORDS, DESCRIPTORS or IDENTIFIERS (technically meaningful terms or short phrases that characterize a document and could be helpful in cataloguing the document. They should be selected so that no security classification is required. Identifiers, such as equipment model designation, trade name, military project code name, geographic location may also be included. If possible keywords should be selected from a published thesaurus. e.g. Thesaurus of Engineering and Scientific Terms (TEST) and that thesaurus-identified. If it not possible to select indexing terms which are Unclassified, the classification of each should be indicated as with the title).

spectrogram segmentation, broadband transient detection, torpedo detection

This page intentionally left blank.

Defence R&D Canada

Canada's leader in defence
and National Security
Science and Technology

R & D pour la défense Canada

Chef de file au Canada en matière
de science et de technologie pour
la défense et la sécurité nationale

www.drdc-rddc.gc.ca